Article

Not peer-reviewed version

# An Ontology of Dirac Fermion of a Monopole Pair (MP) Model of 4D Quantum Space-Time and Its Multifaceted Dynamics

Samuel Yuguru *

Posted Date: 20 August 2025

doi: 10.20944/preprints202210.0172.v18

Keywords: quantum mechanics; quantum field theory; Dirac belt trick; 4D quantum space-time

 doi:10.20944/preprints202210.0172.v18



*Article*

# An Ontology of Dirac Fermion of a Monopole Pair (MP) Model of 4D Quantum Space-Time and Its Multifaceted Dynamics

**Samuel. P. Yuguru**

Department of Chemistry, School of Natural and Physical Sciences, University of Papua New Guinea, P. O. Box 320, Waigani Campus, National Capital District 134, Papua New Guinea; samuel.yuguru@upng.ac.pg; Tel.: +675 326 7102; Fax: +675 326 0369

**Abstract**

In quantum mechanics (QM), the electron of spin-charge in probabilistic distribution about a nucleus of a hydrogen atom is described by non-relativistic Schrödinger's wave equation. Its transformation to Dirac fermion of a complex four-component spinor is incorporated into relativistic quantum field theory (QFT). The quantum system in both cases is represented by a wave function but how it collapses to a point at observation omits out both the hidden variables of the spinor and their evolutionary paths into space-time. This presents an ontological dilemma that cannot be satisfactorily explained by conventional theories either driven by experiments or vice versa. In this study, the ontology of Dirac fermion within a proposed MP model of 4D quantum space-time of hydrogen atom type is examined. The electron of a point-particle and its transformation to Dirac fermion appears consistent with Dirac belt trick (DBT) for the generation of superposition states of spin-charge and their antimatter. Center of mass reference frame owed to DBT offers an alternative version of Newtonian gravity and this is assigned to a specific spherical point-boundary of the model as an emergent geometry. This offers an intricate dynamic tool compatible with basic aspects of both QM and QFT. Some of these are explored for non-relativistic wave function and its collapse, quantized Hamiltonian, Dirac spinors, Standard Model and Lorentz transformation. The space-time geometry of the MP model is presented in the last section and a multiverse of the models at a hierarchy of scales is suggested for a planet in orbit of the sun. These outcomes offer a dynamic intuitive tool that can be modelled and tested for the hydrogen atom in order to probe the fundamentals of physics.

**Keywords:** quantum mechanics; quantum field theory; dirac belt trick; 4D quantum space-time

## I. Introduction

In this section, the rationale for why it is necessary to consider the ontology of Dirac fermion within a boundary of 4D space-time is explored by first outlining the transition of the electron defined by a wave function and its incorporation into both QM and QFT. In section II, the transformation of the valence electron to Dirac fermion by the process of DBT that insinuates the emergence of a spherical MP model of hydrogen atom type is plotted. This defines a center of mass (COM) reference frame of an alternative version to Newtonian gravity and it is assigned to a specific spherical point-boundary of the model. Its intricate dynamics relevant to quantum physics are outlined and these are further explored respectively for both QM and QFT in Sections III and IV. Some of the themes considered include non-relativistic wave function evolution into space-time and its collapse, quantized Hamiltonian, Dirac spinors, Standard Model theory and Lorentz transformation. In Section V, the ontology of the MP model as an emergent geometry for a body-mass in orbit is consolidated for general relativity with respect to space-time fabric, metric tensor and Lie group representation. In the final subsection, an illustration of space-time curvature in a multiverse is

 doi:10.20944/preprints202210.0172.v18



considered for a planet in orbit of the solar system. In Section VI, some concluding remarks on how the model could be tested to probe some basic aspects of quantum physics are mentioned.

*A. Non-Relativistic to Relativistic Quantum Field Theory*

The electron of a point-particle of mass is attributed to $i\hbar$ with $i$ a complex number assigned to a point of a rotating sphere and $\hbar$ to Planck constant of infinitesimal radiation in quantized form [1,2]. The first order space-time derivative of the particle in motion is attributed to non-relativistic Schrödinger equation, $i\hbar\partial/\partial t$ and it is a fundamental concept of particles in QM that cannot be derived by QFT [3]. For light-matter coupling, the energy and momentum operators of Schrödinger equation,

$$\hat{E} = i\hbar\frac{\partial}{\partial t}, \qquad \hat{p} = -i\hbar\boldsymbol{\nabla}, \tag{1}$$

are adapted into QFT beginning with Klein-Gordon equation [4] by second derivation of space-time given in the expression,

$$\left(i^2\hbar^2\frac{\partial^2}{\partial t^2} - c^2\hbar^2\boldsymbol{\nabla}^2 + m^2c^4\right)\psi(t,\bar{x}) = 0. \tag{2}$$

Equation (2) is a relativistic form of Equation (1) and it incorporates special relativity, $E^2 = p^2c^2 + m^2c^4$ by combining momentum and mass. The del operator, $\boldsymbol{\nabla}$ presents 3D space for a particle in motion into space-time. Only one component is considered in Equation (2) and is relevant to describe bosons of whole integer spin and their charges. However, it does not take into account fermions of spin 1/2 and negative energy contribution from antimatter. These are accommodated into the famous Dirac equation [3] of the generic form,

$$i\hbar\gamma^u\partial_u\psi(x) - mc\psi(x) = 0. \tag{3}$$

The symbol, $\gamma^u$ is a set of 4 x 4 gamma matrices, i.e., $\gamma^u = \gamma^0, \gamma^1, \gamma^2, \gamma^3$ and this combines with partial derivative of space-time, $\partial_u = x_0, x_1, x_2, x_3$ to give a scalar quantity which is invariant under Lorentz transformation. The imaginary unit, $i$ unifies space and time according to special relativity and distinguishes 1D time from 3D space by orthonormal relationship for vector space relevant to Clifford group and Clifford algebra, $\mathbb{C} \cong C(0,1)$. The four matrices in $\mathbb{C}(4)$ generate the vector space $C(3,1)$ or $C(1,3)$ and by isomorphism is denoted $\gamma^i$ with respect to Dirac matrices inclusive of a fifth related matrix [5],

$$\gamma^0 = \begin{pmatrix} I & 0 \\ 0 & -I \end{pmatrix}, \qquad \gamma^i = \begin{pmatrix} 0 & \sigma_i \\ -\sigma_i & 0 \end{pmatrix} \Longrightarrow \gamma_5 = \begin{pmatrix} 0 & I \\ I & 0 \end{pmatrix}. \tag{4}$$

The type $\gamma_5 = i\gamma^u$ couples the spinor field, $i$ defined by modes of oscillation, stress-energy tensor and momentum to space-time structure. From Equation (3), the complex four-component spinor, $\psi$ is represented in the form,

$$\psi = \begin{pmatrix} \psi_0 \\ \psi_1 \\ \psi_2 \\ \psi_3 \end{pmatrix}, \tag{5}$$

where $\psi_0$ and $\psi_1$ are spin-up and spin-down components of positive energy with $\psi_2$ and $\psi_3$ as corresponding antimatter for spin-up and spin-down of negative energy. In order to include space-time-energy matrices of the particles, standard Pauli matrix convention is applied such as [5,6],

$$\sigma_0 = \begin{pmatrix} 1 & 0 \\ 0 & 1 \end{pmatrix}, \qquad \sigma_1 = \begin{pmatrix} 0 & 1 \\ 1 & 0 \end{pmatrix},$$

$$\sigma_2 = \begin{pmatrix} 0 & -i \\ i & 0 \end{pmatrix}, \qquad \sigma_3 = \begin{pmatrix} 1 & 0 \\ 0 & -1 \end{pmatrix}. \tag{6}$$

 doi:10.20944/preprints202210.0172.v18



These are a set of 2 x 2 dimensions of complex traceless, Hermitian matrices that are equivalent of involutry and unitary forms. They relate to angular momentum operator of observable spin 1/2 particle respectively in three spatial directions, $\sigma_1$, $\sigma_2$ and $\sigma_3$ with $\sigma_0$ equal to identity matrix, $I$. Any 2 x 2 Hermitian matrices have determinant and traceless values respectively of $-1$ and 0. Their matrix product by linearization is [7],

$$\sigma_i\sigma_j = \delta_{ij}I + i\epsilon_{ijk}\sigma_k, \tag{7}$$

where $\epsilon_{ijk}$ is the Levi-Civita symbol applicable to commutation of cyclic permutation, $[\sigma_i, \sigma_j] = \sigma_i\sigma_I - \sigma_j\sigma_i = i\epsilon_{ijk}\sigma_k$ with anticommutation by combination, $[\sigma_i, \sigma_j] = \sigma_i\sigma_I + \sigma_j\sigma_i = 2\delta_{ij}I$ for $ijk =$ 1,2,3. The orthonormal basis of vector space of 2 x 2 Hermitian matrices over the real numbers, under addition for $\sigma_{13}$ and $\sigma_0$ is the matrix $\sigma_2$ by isomorphism [5],

$$\begin{pmatrix} a & -ib \\ ib & a \end{pmatrix} = a\sigma_0 + b\sigma_{13} \leftrightarrow a + ib. \tag{8}$$

Equation (8) considers real numbers $a \rightarrow \psi_0$ and $b \rightarrow \psi_1$ corresponding to real particles like electron and positron of superposition states. These respectively form real and imaginary parts of $\sigma_2$ based on deterministic outcomes of experiments. The other components $\psi_2$ and $\psi_3$ are attributed to virtual particles, where their creation and annihilation instigates the emergence of real particles. However, how $\psi$ collapses to a point at observation without interactions remains unclear in field theory [8]. In QM, there is no boundary to the evolution of $\psi$ into space-time as described by the generic Schrödinger's equation,

$$i\hbar\frac{d\psi(x,t)}{dt} = \frac{-\hbar^2}{2m}\frac{d^2\psi(x,t)}{dx^2} + V(x)\psi(x,t). \tag{9}$$

The 1st derivative of time is equated to 2nd derivative of space to cater for $\psi$ of probabilistic distributions. Discrete times are not included as this violates the principle of unitary even when these are assigned to virtual particles as in QFT [9]. Bohmian mechanics based on De Broglie wave-particle duality considers virtual particles for the four-component Dirac spinor to be physical as local hidden variables [10]. However, these are completely ruled out by experiments affirming violation of Bell's inequality tests from deterministic outcomes. This is evident in experiments conducted for correlated photon pairs measured either at small distances of 10 km apart [11] or independently from distant astronomical sources [12]. By ruling out locality, plausible quantum gravity-induced entanglement of masses from the hidden variables is invalidated thereby allowing only quantum tests of classical Newtonian interactions [13]. In this case, it is extremely difficult to establish both whether gravity is quantum or classical and the boundary of locality from non-locality towards the big bang [14]. Thus, a proper ontology of $\psi$ is lacking and this cannot be satisfactorily unveiled by both realist and instrumentalist viewpoints offered so far commencing from the Copenhagen interpretation of QM in the early 1900s [15]. It rather requires quantum space-time as opposed to classical space-time dictated by gravity to cater for $\psi$ and this is elaborated next.

*B. Evolution of Dirac Fermion into Quantum Space-Time*

In relativistic QFT, $\gamma^u$ is broken up into four-position coordinates, four-momentum and four-vector for the force in the form [16],

$$\vec{R} = \begin{pmatrix} ct \\ x \\ y \\ z \end{pmatrix}, \quad \vec{P} = \begin{pmatrix} E \\ p_x c \\ p_y c \\ p_z c \end{pmatrix}, \quad \chi^\mu = \begin{pmatrix} x^0 \\ x^1 \\ x^2 \\ x^3 \end{pmatrix}. \tag{10}$$

The components of Equation (10) relate to how $\psi$ permeates space-time and is transformed contravariantly by rotation, translation and inversion. The dominance of matter over antimatter for the four-component spinor as in electroweak baryogenesis [17] is represented in forward time. Antimatter requires time reversal, where discrete times are integrated to space coordinates to

 doi:10.20944/preprints202210.0172.v18



demonstrate violation of charge, parity or their combination in the renormalization process using Feynman diagrams [18]. Antimatter existence by violation of charge conjugation parity is readily observed in both Stern-Gerlach experiment and cosmic rays. In field theory, its intuitive form is represented by Dirac's string trick or belt trick [19], where the electron is converted to a positron at 360° rotation and is restored at 720° rotation. The same is applicable to other related descriptions like Balinese cup trick [20] or Dirac scissors problem [21]. In massless quantum electrodynamics, the electron-positron transition involves creation and annihilation of virtual particles before the emergence of real particles and these are employed by Hamiltonian operators of Hilbert space [22]. However, the likelihood of multiple entanglement states forming for both real and virtual particles towards exponential rise of von Neumann entropy and its boundary from classical Shannon entropy still remains undefined [23]. Whether such distinction can be attributed to quantum arrow of time as opposed to classical time is generally probed for the decay of neutral kaons [24]. It is not clear yet on how space-time can be accommodated into a typical non-radioactive hydrogen atom as primitive matter for its valence electron to comply with Schrödinger's equation. Ionization of hydrogen molecules towards bombardment of clusters of atoms are probed for hadrons collisions in high energy physics. However, without any new insights offered by such experiments, current leading theories still continue to attempt space-time quantization and thus, quantum gravity from a classical perspective of both Newtonian gravity and general relativity.

String theory and its likes consider particles to be made up of strings of different vibrational modes and are contained within multidimensional space-time [25]. Its acceptance as a substantive theory of fundamental physics is yet to be proven in the absence of supersymmetry noted in experiments conducted so far for hadrons collisions [26]. Conversely, both twister approach [27] and loop quantum gravity [28] invoke canonical quantization of gravity by non-commutative spin network of dynamical triangulations to simulate quantum space-time tetrahedra. This might relegate von Neumann entropy of short distance perturbative regime to the nuclei for commutative spin network and this has been successfully trialed in experiments [29] using nuclear magnetic resonance simulator from four $^{13}C$ nuclei. Multiple spinfoam vertex amplitude mimicking angular momenta of space-time tetrahedral are generated and the outcomes look promising for quantum computation to accommodate exponential rise in non-perturbative regimes of vectors in Hilbert space which cannot be easily done by classical computers. However, the most perplexing quest for such novel undertaking and its similar kinds [30,31] in the future is how to probe commutative spin network and to what extent at the atomic nucleus. Perhaps, elucidation of a proper ontology of the atom is needed when experiments have ruled out local hidden variables by Bell's inequality tests in accordance with Copenhagen interpretation of QM. Experimental trials of perturbation theory appear to be quite complex in the investigations of coherence time, superposition and squeeze spin states for quantum gravity-induced entanglement of masses [23,32]. The idea stems from Newtonian potential of dipole moment like electron-positron pairing. On such pursuit, it is still not clear if gravity is quantum with lack of new insights offered both by experiments as mentioned above and from the relationship of black holes and space-time singularities [33], where the tenets of gravity and entanglement are intertwined. Thus, a revisitation to investigate a proper ontology of the hydrogen of one-electron atom appears to be timely in order to begin the quest of establishing a realistic nature of $\psi$ and its adaption into both QM and QFT applications.

### *C. Motivation of This Study*

In this study, Rutherford's atomic model is explored for an electron as a physical entity of a charged point-particle in an elliptical orbit of a MP field mimicking Dirac's string. The electron resembles a monopole in situ of the string as its excitation. Its animation into 3D space is assumed by clockwise precession of the MP field and this generates 1D time so 4D quantum space-time coincides with the emergence of a spherical atomic model. The electron's orbit is of time reversal so an inertia reference frame is induced. It is made compatible to both Schrödinger electron cloud and Bohr models of the hydrogen atom. The transformation of the valence electron to a Dirac fermion is conceived by

 doi:10.20944/preprints202210.0172.v18



the process of DBT into 4D space-time, where superposition states of ±1/2 spin and their antimatter are attained. The COM reference frame relevant to the electron-positron pairing is assigned to the vertex of the MP field at a specific spherical point-boundary. On a geometry basis, both Euclidean and Minkowski quantum space-times are conceived. All these measures offer a multifaceted dynamic tool and it is made compatible to some basic aspects of both QM and QFT. Such a model can be applied to the investigations of the fundamentals of quantum physics at the atomic level and it is worth further considerations.

## II. Ontology of MP Model to Dirac Fermion

Additional details on the conceptualization path of the model from electron wave-diffraction is offered elsewhere [34]. In this section, the transformation of an electron of hydrogen atom type to a fermion by Dirac process within a spherical MP model of 4D space-time is unveiled. First, the rationale for atomic space-time is suggested ensued by how this can be accommodated within the geometry of the MP model by DBT applied on the valence electron. Then the implications for COM and its intricate dynamics at the point of electron-positron transition by DBT are briefly plotted for further pursuits.

### *A. The Rationale for Atomic Space-Time*

The widely accepted model of the atom is the electron cloud model described by Schrödinger's $\psi$. The probability of finding the electron at a time is relegated to orbitals of quantum waves. These are standing waves permeating certain regions of the atom and possess both kinetic and potential energies as demonstrated in Equation (9). The electron in 3D space requires 1D time to account for the shift in its position. Its ontology based on the first principle of space-time derivation (e.g., Equation (1)) cannot be attained by QFT. If applied to the MP model, the MP field undergoing clockwise precession generates 4D space-time of a miniature clockface. This differs from atomic clock [35] which is a collective measure of resonate frequencies of atoms at different heights of potential energy to test the equivalence principle of general relativity. The electron possesses an intrinsic electric charge and its transformation to four-component Dirac fermion is assumed by DBT. The fermion in superposition states of perturbative nature is link to von Neumann entropy and it is separated from Shannon entropy at COM of the spherical point-boundary so quantum space-time is distinct from classical space-time. By energy conservation, entanglement from photons coupled to electron-positron transition is subjected to decoherence to sustain massless bosons. The existence of virtual particles is attributed to the electron-positron transition by DBT so Planck scale elusive in high energy physics [36] is relegated to COM. Gravity is then considered classical and the dipole moment of Coulomb force is attributed to electron-positron transition by DBT. This dipole moment overrides the electrostatic interaction between electron-proton pair for a stable nucleus. These descriptions form the basis to explore a proper ontology of $\psi$ for the valence electron of hydrogen atom.

### *B. Unveiling of Dirac Belt Trick on a Valence Electron*

The geometry of the proposed MP model and some of its emergent features are presented in Figures 1a–d. The electron's orbit in discrete sinusoidal wave form is considered to be of time reversal. In forward time, the orbit is transformed into an elliptical MP field of Dirac's string like a flat miniature magnet. The electron at the vertex mimics a Dirac monopole as quantized state of the MP field of a dipole moment from the electron-positron transition. Clockwise precession generates flat 2D Euclidean space-time of Bohr atomic model (Figure 1a). Perturbations such as nonlinearity of differential gravitation, acceleration between two body-masses, eccentricity of the reference orbit and its oblateness including relative motion of a body-mass in motion against another body-mass are relevant to both Newtonian gravity and general relativity [37]. These are either relegated to the electron-positron transition by DBT or normally considered negligible for a free electron in a valence state. Clockwise precession of the MP field instigates DBT on the

 doi:10.20944/preprints202210.0172.v18



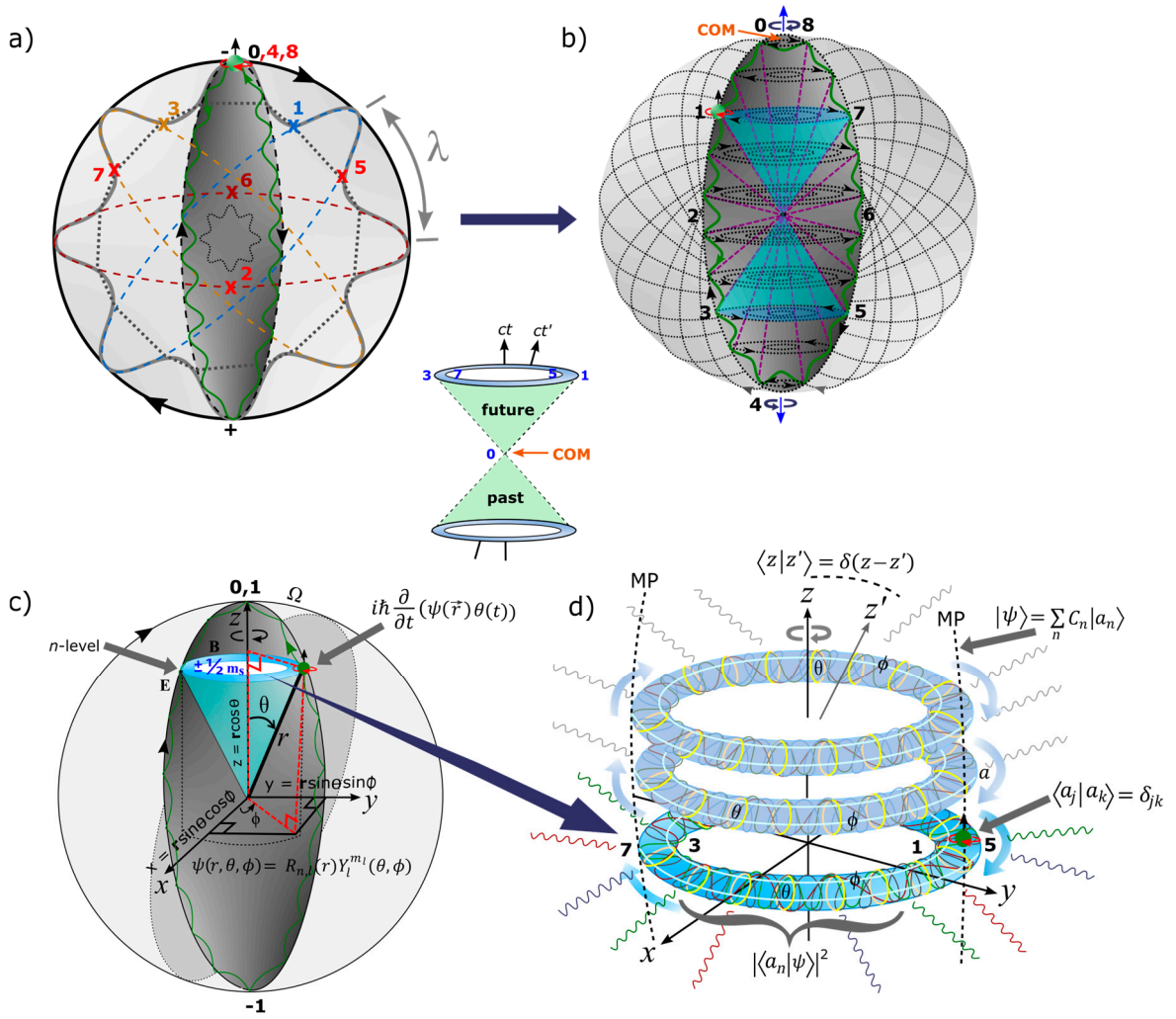


**Figure 1.** The MP model of 4D quantum space-time [34]. (a) In flat Euclidean space-time, quantum time axis in asymmetry is aligned with the principal axis of the MP field. A spinning electron (green dot) in orbit of sinusoidal form (green curve) assumes time reversal and it is normalized to the MP field (black area). Clockwise precession (black arrows) generates an inertia frame, $\lambda$ of a Bohr model type. The electron at position 0 is assigned to COM reference frame of zero-point energy (ZPE) and it is subjected to Newton's first law of motion, $F = ma$. By DBT, the electron shifts in the positions $0 \rightarrow 4$ at 360° rotation and assumes maximum twist. It is converted to a positron to begin the unfolding process from position $5 \rightarrow 8$ for another 360° rotation and the electron is restored to its original state. In the process, a dipole moment (±) of an electric field, **E** is induced between two interchangeable hemispheres of Gaussian-shaped soliton within the MP field. (b) Twisting and unfolding by DBT for the electron-positron transition generates hyperbolic solenoid of spin angular momentum, ±1/2 (navy colored pair of light-cones) into Minkowski space-time. This levitates into $n$-dimensions (purple dotted diagonal lines) of Gaussian soliton (GS) pair from excitation of Bohr model (a) and are linked to smooth manifolds of Bohr orbit (BO) in degeneracy of quantized states aligned perpendicular to the $z$-axis. The helical solenoid of a magnetic field, **B** by unitary is referenced to the hypersurface of the MP field. (c) In a Bloch sphere, the precession stages, $\Omega$, are polarized by the electron-positron transition with qubits, 0 and 1 generated at COM at positions, 0, 8 with determinant -1 attributed to position 4. The polar coordinates (r, θ, Φ) with respect to the electron's position in space are applicable to Schrödinger's wave function. (d) Hyperbolic surface of the light-cone by orthonormal integration of $\phi$ (white loops) and $\theta$ (yellow circles) forms compact topological torus of BO into $n$-dimension by levitation. These are holonomically constrained to a hemisphere of GS. At the vertex, the BO forms hypersurface of Euclidean space and it is configured into clockwise precession of MP field. Balancing out charges at homomorphic positions 1, 3 and 5, 7 becomes isomorphic to BO. Relativistic transformation of COM from the point-boundary (b) to point of singularity of the light-cones (insert image) is accompanied by quantum time

 doi:10.20944/preprints202210.0172.v18



transition, $z - z' \equiv ct - ct'$ into classical time (see also Figures 2a–e). Other embedded terms and equations are described in the text.

electron, where the torque or right-handedness exerted on the vertex at COM shifts the electron of spin up from positions 0 to 4 at 360° rotation. At position 4, maximum twist is attained owed to time reversal orbit against clockwise precession. The electron then flips to spin down mimicking a positron to begin the unfolding process and releases infinitesimal heat friction in the form of Planck radiation, $h$. The positron then shifts from positions 5 to 8 for another 360° rotation to restore the electron at COM and the process of DBT is repeated. Ejection of the electron by ionization induces its particle-hole resonance and is also subjected to DBT with the outcome of $\pm h$ conceived at random. The transition of the electron-positron pairing is restricted to a hemisphere of the MP field resembling Gaussian soliton (GS) and it is interchangeable with the other hemisphere. These are somewhat defined by Heisenberg uncertainty principle, $\Delta x.\Delta p \geq \hbar/2$ for position and momentum conjugate, where the MP field of a dipole moment is consisted of a GS pair. The time lap for the electron transition to positron between the interchangeable GS pair adheres to both Born's rule of square modulus of the wave function, $|\psi|^2$ and Pauli exclusion principle. So, if a GS accommodates the electron or positron by DBT, its devoid GS counterpart assumes the antimatter to accommodate both positive and negative energies. Thus, the Dirac four-component spinor, $\psi_0, \psi_1, \psi_2, \psi_3$ is relatable to the positions 0, 1, 2, 3 from the electron-positron transition. The $z$-axis or principal axis of the MP field equals quantum time and is aligned to COM at position 0 defined by $\psi_0$. From Equation (10), $\gamma^u$ is attributed to clockwise precession and the components, $\vec{R}$, $\vec{P}$ and $\chi^\mu$ to the MP model of flat Euclidean space-time geometry (Figure 1a). Contraction from the 4-gradient covariant term, $\partial_u = \partial/\partial t, \vec{\nabla}$, is assumed by positions $0 \rightarrow 3$ and this complies with unitary at a point in space subjected to the uncertainty principle mentioned above. Thus, any perturbations from COM and mimicked by the vertices of clockwise precession of MP field is referenced to an inertia reference frame, $\lambda$ (Figure 1a) under the conditions,

$$\lambda_\pm^2 = \lambda_\pm, \quad Tr\lambda_\pm = 2, \quad \lambda_+ + \lambda_- = 1, \qquad (11)$$

where the trace function, $Tr$ is the sum of all elements within the model. This serves as an avenue to explore its relevance to both QM and QFT applications from the onset of the model at COM.

*C. COM Reference Frame and Its Intricate Dynamics*

The COM reference frame on a specific spherical point-boundary is at the interface of classical and atomic states. Somehow, it merges both Einstein geometry of space-time curvature by clockwise precession of the MP field and Newtonian gravity of a dipole moment at the singularity of Hilbert space. Precession determines how the electron of a body-mass should move and in turn, its motion in orbit by DBT dictates how the model should curve for observations limited to light-matter coupling. This has important implications to quantum physics and some of them are succinctly outlined in here.

- For quantum gravity assigned to COM, it differs from the orthodox interpretation of classical Newtonian gravity. The electron-positron transition by DBT is isomorphic of two body-masses coupling at a distance. It is of ZPE and the spinor formed from the electron shift in positions 0 to 3 of superposition states encompasses local hidden variables with observational outcomes mimicking Bell's inequality tests. In situ of the atom, the variables can relate to quantum gravity-induced entanglement of masses in low energy setting [13,23,31] of generalized Stern-Gerlach interferometers. For example, the electron-positron pair of coherent state is assumed at COM (Figure 2a). By homomorphism, it is partitioned to electron-positron transition, $\psi_0 \rightarrow \psi_3$ of superposition states into 4D quantum space-time (Figure 2b). Squeezing the two spin states at COM is conceived at 360° by DBT, where the electron is converted to a positron at maximum twist (Figure 2c). The unfolding process at another 360° restores the electron to its original state. In this case, vertical to horizontal polarization or vice versa for the electron-positron transition

 doi:10.20944/preprints202210.0172.v18



supersedes the electron-proton electrostatic interaction. For an irreducible spinor of the MP model, ejection of the electron by ionization is expected to generate its particle-hole resonance structure of invariant behavior akin to those observed in condensed matter physics. Coupling of the particle-holes or protonized hydrogen atoms in high energy regime allows for the development of scattering matrix by shortening of BOs into $n$- dimensions under the natural setting, $n_\infty = \varepsilon_0 = c = \hbar = 1$ (Figure 2d). From vertical to

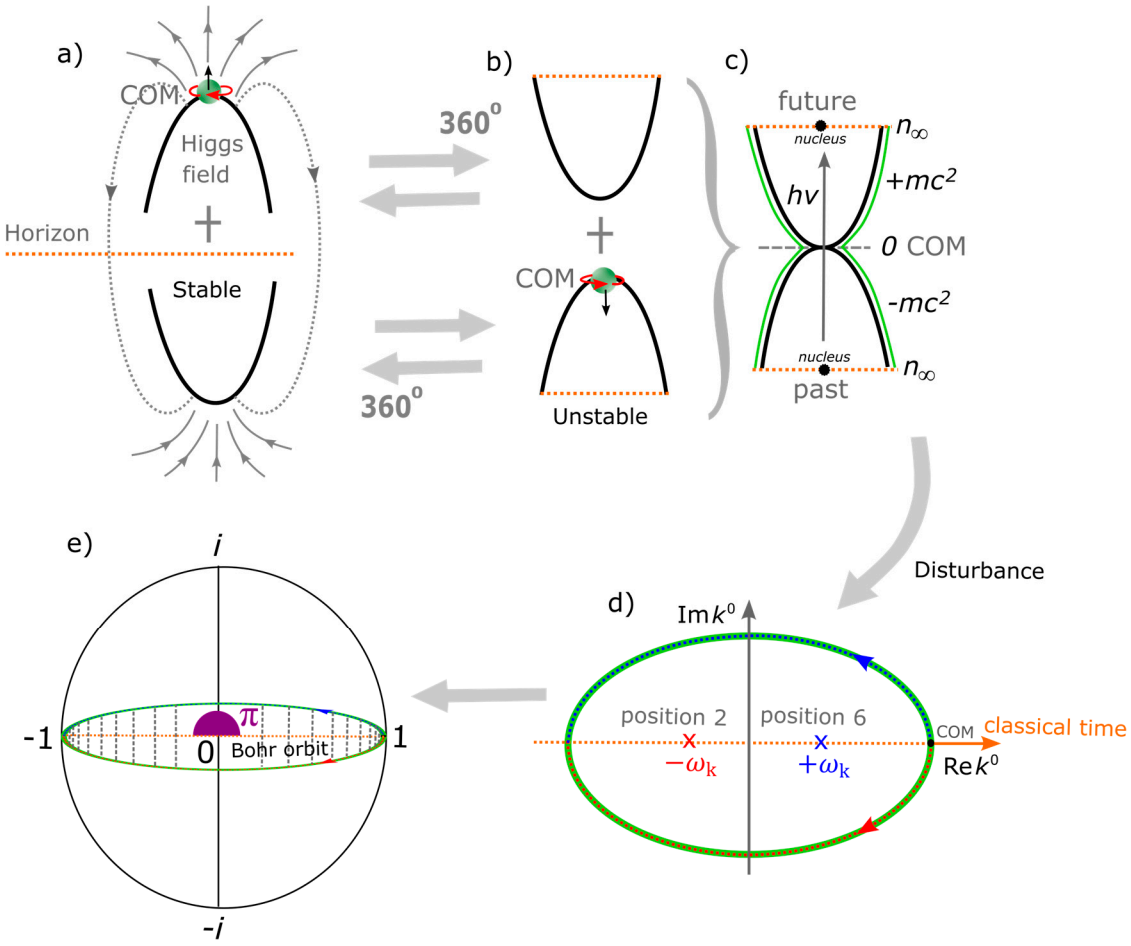


**Figure 2.** COM reference frame and its polarization. (a) Under clockwise precession, the monopole or electron at the top vertex is compelled towards the unoccupied bottom vertex by the process of DBT to induce a dipole moment akin to a miniature magnet. The vortex electron's path is solenoidal between the GS pair of Born's squared wave function (see also Figure 1a). (b) At 360° rotation the electron is subjected to maximum twist and the combined GS pair of hyperbolic geometry evolves into an oscillation mode. (c) The electron or its particle-hole resonance of ZPE forms vacuum expectation value of Higgs boson type with the GS pair mimicking one Higgs doublet amplitude. Electroweak symmetry breaking for the unfolding process is initiated at COM to instigate either positive or negative scalar field potential. (d) The perturbative field is quantized, $E = nh\nu$ into BOs of $n$-dimensions intersected by the electron's path and this coincides with the emergence of a pair of light cones. (d) Another 360° rotation and the hyperbolic GS pair is restored. The process of DBT resembles vertical to horizontal polarization to induce a dipole moment. The where the scattering matrix from shortened BOs of an elongated Hadron-jet like mode is terminated at COM. (e) Any outgoing radiation acquires quantized mass and the MP model of Dirac spinor obeys Euler's identity on conventional Pauli matrices, 0, –1 and 1 assumed at COM respectively at positions 0, 4 and 8 (see also Figure 1a).

horizontal polarization, the strong coupling strength, $\alpha_5$ from oscillations of fermions and bosons at the potential wells of ZPE vanishes (Figure 2c). Quarks and gluons are freed and interact weakly with each other in accordance with the property of asymptotic freedom [38]. Unitary for

 doi:10.20944/preprints202210.0172.v18



gauge symmetry defined by Euler's identity, $e^{i\pi} + 1 = 0$ for an atom of Bloch sphere allows for the development of quark flavor and color confinement (Figure 2e).

- The electron or its particle-hole is likened to either Dirac monopole or Higgs boson at COM of Planck length (Figure 2a). The monopole is assumed at the vertex and it is converted to a Higgs at 360° rotation and back to a monopole at another 360° to complete the process of DBT. Mass acquisition by oscillation is at the potential well of ZPE resembling vacuum expectation value and is subjected to light-matter coupling. Oscillation of the GS pair resembles one Higgs doublet field, $\pi/2$ (Figure 2b) and this is reduced to the point of singularity at COM (Figure 2c). Maximum twist and unfolding process by DBT breaks the symmetry with the release of infinitesimal Planck radiation at random. In low energy setting, any disturbance by excitation promotes BOs of $n$-dimensions into the quantized form, $E_n = \left(n + \frac{1}{2}\right)\hbar\omega$. The GS accommodating the electron of quantized states is balanced out by its interchangeable unoccupied GS counterpart. The oscillation overrides any radiation from a stable nucleus and the perturbation terminates at COM at the interface of quantum and classical levels in accordance with the correspondence principle (Figure 2c). The hydrogen spectrum, $E_n = \frac{1}{2}\hbar\omega$ is about 13.6 eV for ZPE. The emergence of wave amplitudes at the $n$-levels from light-matter (electron) coupling is dictated by the uncertainty principle. At high energy, the quantized states of BOs into $n$-dimensions are shortened to form elongated Hadron-jet like mode. Mixing at positions 2 and 6 inclusive of compacted BOs at higher dimensions can become massive akin to Nambu-Goldstone boson types (Figure 2d). The outputs at COM of Higgs boson type are attained at $r = 0$ from vertical to horizontal polarization or vice versa. Particle emergence by mass acquisition, $m = E/c^2$ is conceived from shortening and mixing of BO of $n$-dimensions of quantized states, $E = nhv$ (Figure 2c). Decoherence is expected from colliding energized light waves for massless photons.
- The electron in perpetual motion acquires angular momentum at positions 1 and 3 of the GS pair and exhibits the centrifugal force, $F_c = G(mv^2/r)^2$ of Newton potential. For the free electron, its nuclear attractive force, $F_e = e^2/4\pi\varepsilon_0 r^2$ is assumed by DBT. The shift in COM of Higgs type to the center resembles Coulomb force, $F_e = k_e q_1 q_2/r^2$, with $k_e$ equal to the dipole moment of the MP field and $q_1 q_2$ to electron-positron pair. The vertices of COM by clockwise precession are translated linearly into the intervals, $x + dx$ with the emergence of the monopole or electron at random. Non-linear shift in the electron's position by DBT generates qubits, 0, –1 and 1 at COM to sustain unitary. The continual clockwise precession of the MP field of 2D and its translation to 4D space-time can relate its COM to both gravitational horizon and the holographic principle. Von Neumann entropy is linked to the electron-positron transition of superposition states at quantized states of BOs into $n$-dimensions. The GS pair provides both matter and antimatter types and it allows for quantum tunneling and this can be differentiated from classical Shannon entropy at COM.
- The electron in orbit of 4D space-time with respect to $z$-axis provides a proper ontology of space-time derivation, $i\hbar\frac{\partial}{\partial t}\left(\psi(\vec{r})\theta(t)\right)$ from the first principle (see also Figure 1c). The electron-positron spin-charge of superposition is relatable to Schrödinger's cat narrative and the model offers an advanced version of Schrödinger's cloud model. The basis vectors, $\vec{r}$ and $\theta$ for BO are aligned to $x$-$y$ plane and orthonormal to $z$-axis (e.g., Figure 1c). The electron's orbit can be split into both radial and angular wave components, $\psi(r,\theta,\phi) = R_{n,l}(r)Y_l^{m_l}(\theta,\phi)$. The radial part, $R_{n,l}$ is attributed to the principal quantum number, $n$ and this is linked to BO. The angular momentum, $l$ is assigned to a light-cone at distance, $r$ from the nucleus (Figure 1c). The angular part, $Y_l^{m_l}$ of degenerate states, $\pm m_l$ with respect to $\theta$ and $\phi$ are assigned to BOs of topological torus (e.g., Figure 1d). The inner product, $\langle\psi|\phi\rangle^* = \langle\psi|\phi\rangle$ of GS pair can relate to second derivative of space, $\frac{-\hbar^2}{2m}\frac{d^2\psi(x,t)}{dx^2}$.
- The charge-parity-time symmetry appears invariant at COM for time aligned to $z$-axis. Symmetry is conserved for both multidimensional Euclidean and 4D Minkowski space-times

 doi:10.20944/preprints202210.0172.v18



(Figures 1a and 1b). At 360° rotation, electroweak symmetry breaking for combined charge conjugation and parity inversion of hyperbolic GS pair institutes vacuum expectation value of ZPE (Figure 2c). This is accentuated by the externally applied energies with the mixing and output from a point-spread Green function linked to COM (Figure 2e). The light-MP model coupling tangential to the model at COM is relevant to Fourier transform of electromagnetic waves [39]. The generated electric field, $\nabla . E(\psi) = -\partial B/\partial t(\psi) = m_j \hbar(\psi)$ at COM relates to a Dirac monopole, $\nabla . B(\psi) = 0$ (Figure 2a). By DBT, the vortex electron evolves into solenoid loops of instantons for the GS pair in the polarized state, $\nabla . E\ (\psi) = \rho/\varepsilon_0(\psi)$ with $\rho$ equal to BO of $n$-dimensions and $\varepsilon_0$ to the dipole moment of the MP field. The solenoid path is essential to the application of Ampere-Maxwell circuit law, $\nabla . H = J + \partial D/\partial t$ with $J$ attained at positions 1 and 3. Propagators from signal processing from the center to the boundary (Figure 2d) form integral kernels of Greens function like the wave operator, $\psi = Ae^{+ikx} + Be^{-ikx}$. Klein-Gordon operator, $\partial^\mu \partial_\mu \phi = 0$ is assumed for the emergence of the hyperbolic surface of the light-cones and its restoration at COM (e.g., Figures 2c–e). The Klein-Gordon Greens function, $\partial^\mu \partial_\mu \phi G(x - y) = \delta^4(x - y)$ is of 4D space-time and this can relate to the massless scalar Higgs field of second-order space-time. Its Dirac delta function, $\delta^4$ integrates scattering matrix with the output at COM (Figure 2d). The output of sine wave function can be both homogeneous and inhomogeneous waves. The former from spherical boundary of GS pair and the latter to electron's position shift about the light-cones. Cosine waves of non-linearity is expected from the electron's shift in position away from COM. Other relatable Fourier transforms for mixing at COM include invariance commutation plus propagators of casual and retarded Feynman path integral.

- The COM offers singularity of Hilbert space into Minkowski space-time and initiates the magnetic dipole moment, $u$ by DBT (e.g., Figure 2c). The spaces of inner product to vector, metric and topology of $n$-dimensions can be envisioned for the BO into $n$-dimensions (e.g., Figure 1d). These are confined to moduli of vertices by continuity of precession and this generates infinite Hamiltonian spaces of virtual particles, i.e., $P(0 \rightarrow 8) = \int_\tau^{\square} \psi^* \hat{H} \psi d\tau$ with time equal to $\tau$. The Hermitian is represented by GS of a hemisphere constituting an electron in orbit and its interchangeable non-Hermitian to the GS counterpart devoid of the electron. Integration of Planck theory and Einstein mass-energy equivalence of the relationship, $\lambda = h/mv$ of wave-particle duality is forged within the model. Commutation of electron-electron pair is attained at 720° and anticommutation at 360° rotation. The former offers an inertia frame and the latter can relate to the form [40], $\langle a_j | a_k \rangle = \int dx \psi^*_{a_j}(x) \psi_{a_k}(x) = \delta_{jk}$. The sum of expansion coefficients, $C_n$, by continuity of precession renders the expectant value, $|\psi\rangle = \sum_n C_n / a_n\rangle$ and its probability, $\langle a_n | \psi \rangle^2$.

The COM is shown to be quite dynamic and is able to integrate many basic aspects of QM and QFT into a proper perspective. Some of these themes are more complex to unveil by mathematical approach without having a proper intuitive guide. The MP model offers one tangible way to guide physics in general by providing a realistic intuitive tool.

## III. Ontology of MP Model to Quantum Mechanics

The attributes of the MP model towards QM are explored into three parts. First, the non-relativistic aspect of $\psi$ is presented ensued by its collapse at observation. Third, some perspectives on quantized Hamiltonian are presented with respect to how perturbations is attained by DBT and this terminate at the COM on the vertex of the MP field.

### *A.Non-Relativistic Wave Function and Its Attributes*

In theory, a key difference between classical and quantum oscillators is incorporated by Schrödinger's wave equation and it forms the basis of QM. Despite its tremendous success, QM still cannot fully account for the combination of orbital angular momenta, $\vec{l}$, spin angular momenta, $\vec{s}$

 doi:10.20944/preprints202210.0172.v18



and magnetic moments, $\vec{m}$ of valence electrons observed in atomic spectra [41]. Similarly, how both integers to half-integers spins are accommodated by relativistic transformation of $\psi$ from QM to QFT remains oblivious. The ontology of $\psi$ for the Dirac fermion is previously demonstrated in Section IIB (see also Figures 1a–e). Its non-relativistic attributes on a geometry perspective with respect to the MP model are provided in Figures 2a–e. How all these are aligned to the energy shells of BOs at $n$-levels and incorporate $l$, $s$ and $m$ and other related attributes are explored in this subsection. This further extends to how perturbations from light-MP model coupling could account for Lamb shift and thus, fine-structure constant, $\alpha$ of hydrogen spectral lines among a few others.

In Figure 3a, the levitation of BO into $n$-dimensions for complex fermions of ±1/2, ±3/2, ±5/2 and so forth is conceived for light-matter(electron) coupling at positions 1, 3 and their conjugates positions of 5, 7 (see also Figure 1d). Infinite $n$-dimensions extend towards the boundary of the hyperbolic surface for the GS pair dissecting the nucleus (Figure 2c) and by asymptotic freedom, this overrides any perturbations of a stable nucleus. Oscillations of the MP model is quantized from the electron-positron transition by DBT and the emergent light-cones of superposition states are linked to acquisition of angular momenta at positions 1 and 3 (Figure 3b).

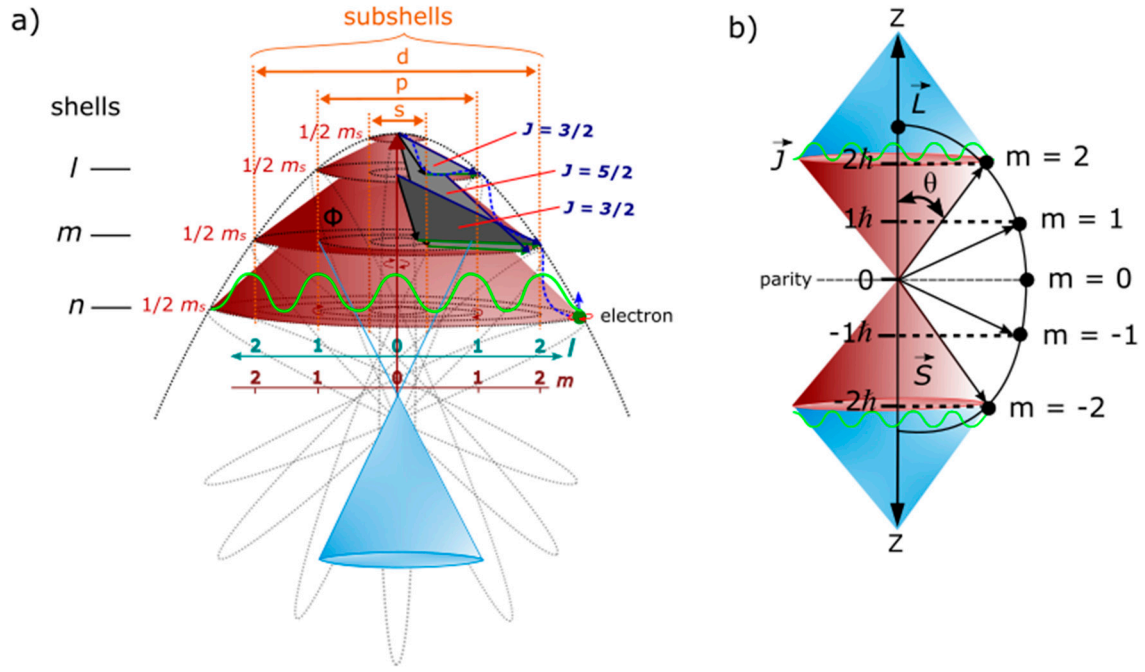


**Figure 3.** Quantum oscillators of GS pair. (a) The emergence of quantum oscillators (maroon light-cones) is linked to COM of topological point-boundary (see also Figure 2c). Total angular momentum, $J_z = S + L$ is applicable to the light-cones within the GS pair. Extension of BOs into $n$-dimensions from $n_\infty$ to $k$ terminates at COM at the interface of atomic and classical scales in accordance with the correspondence principle (see also Figure 2d). The BOs in degeneracy, $\Phi_i$ of $n$-dimensions are assigned spectroscopic notations, s, p, d and so forth. These are applicable to Fermi-Dirac statistics (green wavy curve) and Fock space for non-relativistic many-particle systems supposing the spherical atom is a replica of multielectron atom for each electron assigned to a MP field. Emergence of blue light-cone at the completion of DBT is pertinent to balancing out of non-relativistic Schrödinger wave function (e.g., Figure 1c). (b) Superposition states, $\pm J_z = m_j \hbar$ is applicable at $n$-dimensions of the GS pair (see also Figure 2c).

It is important to note that at perturbation, the COM coincides with singularity at the nucleus by squared wave function of GS pair amplitudes (Figure 2c). Thus, Planck radiation from COM at random will appear to be instigated at the nucleus. But instead, it actually emanates from the electron-positron transition at the spherical point-boundary. The electron possesses intrinsic spin and its

 doi:10.20944/preprints202210.0172.v18



orbital angular momentum is quantized, $s = 1/2\hbar$. The magnitude from Russell-Saunders orbital-spin (L-S) coupling takes the form,

$$|\mathbf{L}| = \sqrt{\mathbf{L}_\mathrm{n}(\mathbf{L}_\mathrm{n}+1)}\hbar, \qquad (12a)$$

where $\mathbf{L}_\mathrm{n}$ is attributed to the electron's position at positions 1 and 3 of BO into $n$-dimensions by levitations. It is linked to degenerate states of subshells. The resultant **L** is of the values, 0, $\sqrt{2}\hbar$ and $\sqrt{6}\hbar$ respectively for $n = 0$, $n$ =1 and $n = 2$ (Figure 3b). Their projection about $z$-axis for an irreducible spinor of the MP field is,

$$|\mathbf{L_Z}| = M_L\hbar, \qquad (12b)$$

where $M_L$is the magnitude of the BO. In vector space of the hyperbolic surface of a light-cone, $L_z$ is translated to $J_Z$ by,

$$J_Z = m_l\hbar, \qquad (12c)$$

where $m_l$ can take the values, $2l + 1$ from the subshells or degenerate states of BO as eigenfunction of $M_L$. Further distinctions between these parameters are provided in Figures 4a for $J^*$ not aligned to $z$-axis with $|m| < \sqrt{j\,(j+1)}$ (Figure 4b). These are necessary for quantization of infinitesimal space for $z$-axis equal to quantum time. These explanations can relate to Lamb shift in the following manner.

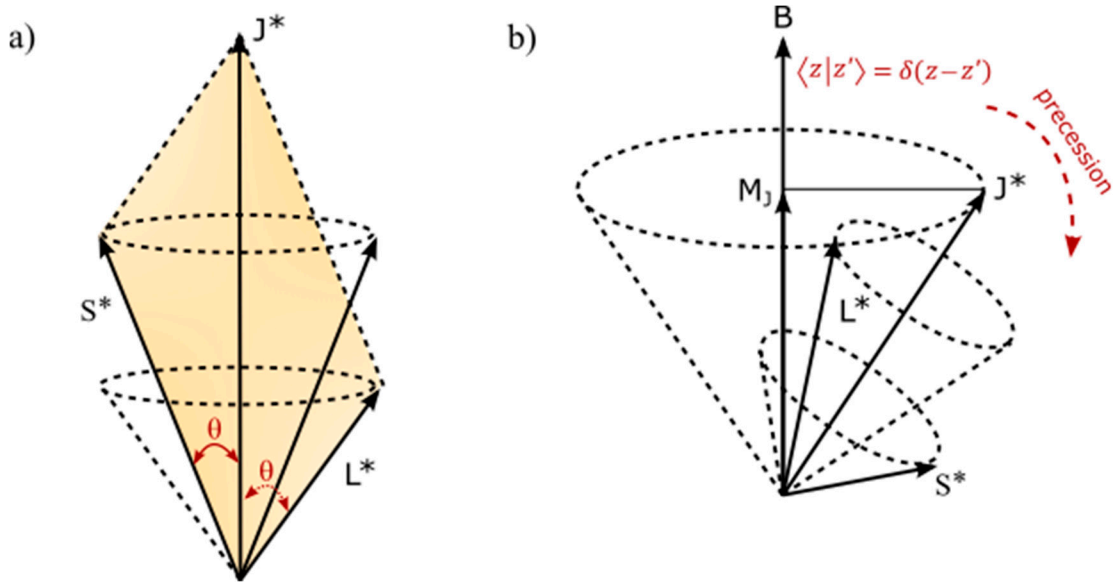


**Figure 4.** Vectors of angular momentum. (a) **J** results from precession of vectors **L** and **S**. The shaded area of bivector is extended to COM at the point-boundary of the spherical model (see also Figure 3a). (b) Precession of **J** of hyperbolic surface in Minkowski space-time can be accentuated by applied external magnetic field **B**. Both images are adapted and slightly modified from ref. [41].

At $n = 2$, $l = 1$, this is split into $s$ and $p$ orbitals, each one accommodating ±1/2 spin from the electron-positron transition by DBT. The total angular momentum, $\vec{J} = l \pm \frac{1}{2}$, equates to $\frac{3}{2}$ and $\frac{1}{2}$ . If applied to Figure 3a, the summation of spin, 1/2 + 1/2 + 1/2 is made from combined $s$ and $p_{x,y}$ subshells at $n_2 + n_1 = \frac{3}{2}$ . It combines $l = 1$ at positions 1 and 3 of BO to $l = 0$ at position 0. The $p_z$ subshell is indistinguishable from $s$ subshell for the vector axis aligned with $z$-axis. That is both $s$ and $l$ are in the same direction and of low energy. The resultant spin angular momentum, **S** of a light-cone is referenced to COM at singularity (see also Figure 2c). For $n_2 - n_1 = \frac{1}{2}$, it is given by, 1/2 +1/2 −1/2 (Figure 3b). The combined $p_z$ and $s$ subshells for spin down of $z$-axis are subtracted from $p_{x,y}$

 doi:10.20944/preprints202210.0172.v18



subshells. So, the Lamb shift spacing of 0.035cm$^{-1}$ between $^2S_{1/2}$ and $^2P_{1/2}$ is applicable to ZPE fluctuations at COM. Twisting and unfolding from DBT accommodates $\pm i\hbar$ with respect to position and momentum (e.g., Figure 2c). The COM can further relate to, $\alpha = e^2/4\pi \approx 1/137$. Fine-tuning of $\alpha$ is an artifact of the effects of DBT and this is pertinent to the anomalous magnetic moment, $a_e = a/2\pi$. Similarly, the acquired $J_z$ by rotation or precession of MP field space at positions 1 and 3 is relevant to the calculation of the gyromagnetic ratio or $g$-factor, $\gamma = u/|J_z|$ or $\gamma = 2a_e + 2$. Any exponential increase in quantum perturbation from moduli of vertices and $\pm\vec{J}$ splitting for Landé interval rule from on-shell momentum are mixed with output of Fourier transform assumed at COM (Figure 2e). These explanations might shed some insights into Zeeman effect of odd spin types and the refinement of Rydberg constant [42], $R_\infty = a^2 m_e c/2h$ for the hydrogen atom in terms of proton radius puzzle. Similarly, the envelop solitons of hyperbolic surface at positions 2 and 6 (Figure 2c) could restrict accessibility to the nucleus and this can become important in the quest of constraining quantum critical point [43] for Rydberg atom arrays of ferromagnetism resembling multiple MP models. Such intuitive insights could become important in low energy physics applications.

*B. Wave Function Evolution into Space-Time and Its Collapse*

Dirac fermion of a four-component spinor is denoted $\psi(\mathbf{x})$ in 3D Euclidean space. Quantum time is trivial, $(z - z') = \langle z|z'\rangle$ in flat space (Figure 1a) and is absorbed into classical time, $ct - ct'$ at COM (Figure 2d). The distance between any two events is always positive like position 2 and 6 in space as given in the form [44],

$$ds^2 = dx^2 + dy^2 + dz^2 = (x_2 - x_1)^2 + (y_2 - y_1)^2 + (z_2 - z_1)^2. \quad (13)$$

Once the electron acquires spin angular momentum by DBT, Euclidean space-time is transformed into 4D Minkowski space-time, $\psi(\mathbf{x},t)$ (e.g., Figure 1b). The hyperbolic space of the light-cone of both inertia and accelerated reference frames is subject to Lorentz transformation of time invariance [44],

$$ds^2 = dx^2 + dy^2 + dz^2 - ct^2. \quad (14)$$

Both Equations (13) and (14) appear independent of a stationary observer with respect to the electron probability distribution as demonstrated in Figures 2a–e. The orthonormal shift identifies with vertical to horizontal polarization. The emergence of the pair of light-cones coincides with Minkowski space-time and these are dissected by $z$-axis of quantum time in asymmetry. In non-Euclidean space, both positive and negative curvatures from the electron-positron transition are normalized to straight paths of Euclidean space (Figure 5a). Convergence of quantum space-time at COM (e.g., Figure 2c) is relevant to the equivalence principle for Euclidean space superimposed on the surface of the spherical MP model mimicking a Bloch sphere (Figure 5b). In such a case, the

Preprints.org (www.preprints.org) | NOT PEER-REVIEWED | Posted: 20 August 2025 doi:10.20944/preprints202210.0172.v18



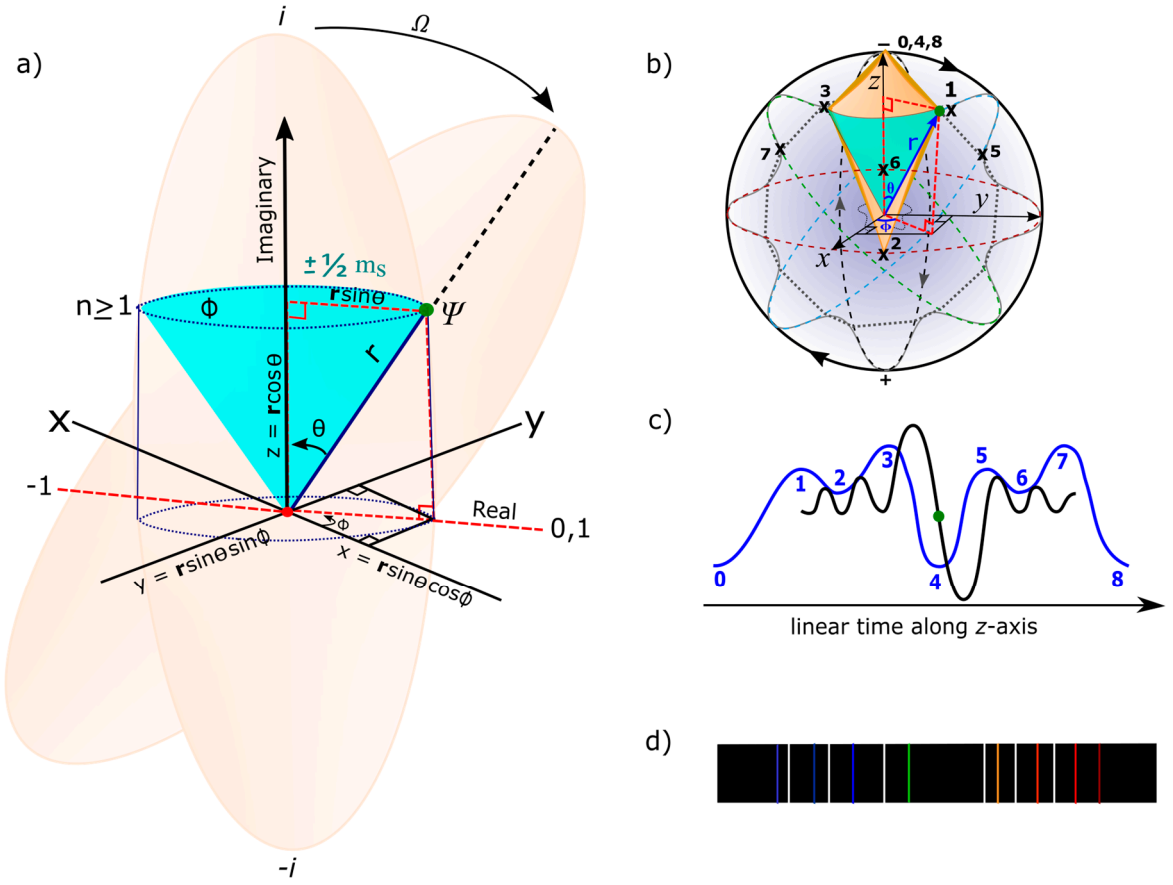


**Figure 5.** Evolution of the wave function into space-time and its collapse. (a) At clockwise precession, the irreducible MP field of Dirac's string incorporates the electron's shift in position by DBT. The particle at a diagonal line, $r$ is assigned the polar coordinates (r, θ, Φ) and is linked to a light-cone (navy colored). Its acquisition of angular momenta either at positions 1 and 3 or 5 and 7 is relevant to Euler's formula, $e^{i\pi} = cos\pi + isin\pi$ with $\theta = \pi$ (see also Figure 2e). The real part, $cos\pi$ is aligned to $x$-$y$ plane and the imaginary part, $isin\pi$ to $z$-axis. Unitary, $|\psi|^2 = x^2 + y^2 = 1$ is sustained and qubits, 0, 1 and -1 are generated at COM of position 0. (b) Vector space of Dirac spinor (shaded yellow) is superimposed on a Bloch sphere. It consists of both Euclidean (straight paths) and non-Euclidean (negative and positive curves) spaces. (c) On-shell momentum of BO intersected by the electron's path is compatible with hydrodynamic pilot-wave system of a quantum particle possessing internal vibration at twice the Compton frequency [45] comparable to Fourier transform (blue wavy curve) of the GS pair. The position is undefined based on Heisenberg uncertainty principle (black wavy curve). Their translation to linear time for light waves-electron coupling mimics (d) a typical hydrogen emission spectrum from the ground state to infinite $n$-dimension and this can accommodate Humphery to Lynman series (see also Figure 2e).

quantum aspect of de Sitter space by geodetic clockwise precession is balanced out by anti-de Sitter form of the electron transition in its orbit of 4D quantum space-time. The combined metric for the two space-time spheres of Euclidean and Minkowski, $S^2$ at radius, $\alpha$ is given by,

$$ds^2 = a^2(d\theta^2 + sin^2\theta d\phi^2 ). \qquad (15)$$

Equation (15) is applicable to linear Fourier transform at COM on a 2D sphere (e.g., Figure 2e). The two operators, $T_a$ and $S_a$ acting on vector space becomes,

$$(T_a f)(b) = f(b - a) \qquad (16a)$$

and

 doi:10.20944/preprints202210.0172.v18



$$(S_a f)(b) = e^{2\pi i ab} f(b), \tag{16b}$$

where $T$ is identified by the rotational matrices, $T = \vec{r} \times F$ and $S_a$ is the shift in frequency in space by outsourcing at COM. Perturbation of the model is self-initiated by electron-positron transition of DBT at COM of ZPE and it is orthonormal to light-electron coupling (Figure 2d). The four-component spinor, $\psi_{0\to3}$ with respect to the electron's orbit is reduced to two-component bispinor of superposition state in the form,

$$\psi = \begin{pmatrix} \psi_0 \\ \psi_1 \\ \psi_2 \\ \psi_3 \end{pmatrix} = \begin{pmatrix} u_+ \\ u_- \end{pmatrix}. \tag{17}$$

The Weyl spinors of chirality, $u_\pm$ of angular momenta are linked to the pair of light-cones into Minkowski space-time (Figure 5a). The spin up and spin down fermions (i.e., $\psi_0$, $\psi_1$) corresponds to the particle's position at the occupied GS of squared amplitude towards 720° rotation. The antifermions of both spin up and spin down ($\psi_2$ and $\psi_3$) are formed on the accompanied unoccupied GS as previously mentioned. The moduli of vertices on the MP field at clockwise precession are relevant to the creation and annihilation operators $\gamma(E), \gamma^\dagger(E)$ of virtual particles. For Fermi level $\gamma(0) \equiv \gamma = \gamma^\dagger$ assigned to COM of ZPE, the fermion is promoted to the conductance band of higher $n$-dimensions towards elongation of the model (e.g., Figure 2d). The anticommutation relation at 360° rotation is given by [46],

$$\gamma_n \gamma_m + \gamma_m \gamma_n = 2\delta_{nm}. \tag{18}$$

The product of Equation (18), $\gamma_n^2 = 1$ is assumed at 720° from combined oscillators of bosonic field. Duplication of Lamb shift at COM on the vertices of the MP field by clockwise precession combined with BO of $n$-dimensions could provide Hamiltonian spaces for both hydrogen emission spectrum (Figure 5d) and scattering matrix of wave amplitudes. Constraining the electron's position towards COM is defined by $i\hbar$. Thus, the MP model offers a primitive ontology of $\psi$ somewhat related to both Bohmian mechanics that has remained elusive [47] and the enigmas of fluctuations of quantum fields [48]. Experimental outcomes of superposition states from the electron-positron transition at positions $0 \to 3$ in repetition is expected to somehow obey both Stern-Gerlach experiment and Bell's inequality tests.

*C. Quantized Hamiltonian*

Two ansatzes adapted from Equation (3) are given by,

$$\psi = u(\mathbf{p}) e^{-ip.x}, \tag{19a}$$

and

$$\psi = v(\mathbf{p}) e^{ip.x}, \tag{19b}$$

where outward projection of electron spin is of $v$ type and inward projection of $u$ type. Equations 19(a) and 19(b) can relate to the GS pair of oscillation mode from the electron-positron transition by DBT within a Hamiltonian spherical model. The $v$ type projection can be attributed to clockwise precession from positions $0 \to 3$ and the $u$ type to positions $4 \to 8$. The exponential increase in the electron-positron distribution of uncertainty is attributed to the MP model. Linear transformation for quantum time is merged into classical time at COM and this can accommodate Hermitian plane wave solutions as the basis for Fourier components in 3D space (e.g., Figures 2d and 5c). Decomposition of quantized Hamiltonian then becomes [49],

 doi:10.20944/preprints202210.0172.v18



$$\psi(x) = \frac{1}{(2\pi)^{3/2}} \int \frac{d^3}{2E_{\mathbf{p}}} \sum_s \left( a_{\mathbf{P}}^s u^s(p) e^{-ip.x} + b_{\mathbf{P}}^{s\dagger} v^s(p) e^{ip.x} \right), \tag{20a}$$

where the constant, $\frac{1}{(2\pi)^{3/2}}$ is attributed to GS pair accommodating Lamb shift at the potential wells described in subsection IIIa with respect to Figure 3a. Its conjugate is,

$$\bar{\psi}(x) = \frac{1}{(2\pi)^{3/2}} \int \frac{d^3}{2E_{\mathbf{p}}} \sum_s \left( a_{\mathbf{P}}^{s\dagger} \bar{u}^s(p) e^{ip.x} + b_{\mathbf{P}}^s \bar{v}^s(p) e^{-ip.x} \right). \tag{20b}$$

The coefficients $a_{\mathbf{P}}^s$ and $a_{\mathbf{P}}^{s\dagger}$ are ladder operators for $u$-type spinor and $b_{\mathbf{P}}^s$ and $b_{\mathbf{P}}^{s\dagger}$ for $v$-type spinor. The operators are applicable to BOs of topological torus into $n$-dimensions linked to the electron-positron transition. The spinors of two spin states, ±1/2 are accompanied by their respective antiparticles, $\bar{v}^s$ and $\bar{u}^s$. These are attributed to the electron-positron transition within the GS pair, where the interchangeable devoid component assumes the antimatter role as previously mentioned. Apart from outgoing Planck radiation of frictional mode from the twisting and unfolding process by DBT at COM from either the electron or its particle-hole resonance, the hydrogen atom is conserved. The Dirac Hamiltonian of its one valence electron is [50],

$$H = \int d^3x \psi^\dagger(x) [-i\boldsymbol{\nabla}.\boldsymbol{\alpha} + m\beta] \psi(x), \tag{21}$$

where the electron, $i$ acquires vectors of momentum, $\nabla$ by shift in its position with Dirac's gamma matrices attributed to positions $0 \rightarrow 3$ of superposition states accorded to the standard Pauli matrices, $\alpha$, $\beta$. The associated momentum becomes,

$$\pi = \frac{\partial \mathcal{L}}{\partial \psi} - \bar{\psi} i\gamma^0 = i\psi^\dagger. \tag{22}$$

The Lagrangian, $\mathcal{L}$ from Equation (22) is attempted from clockwise precession that instigates the electron-positron transition towards COM represented by $\bar{\psi}$ and of position 0 depicted by $\gamma^0$ with respect to $z$-axis as quantum time. Projection of the electric currents in the $x$-$y$ directions is analogous to Fourier transform from vertical to horizontal polarization (e.g., Figure 2d). The outcome of the superposition states from positions $0 \rightarrow 3$ and their antimatter gives the following relationship [51],

$$\left[ \psi_\alpha(\mathbf{x}, t), \psi_\beta(\mathbf{y}, t) \right] = \left[ \psi_\alpha^\dagger(\mathbf{x}, t), \psi_\beta^\dagger(\mathbf{y}, t) \right] = 0. \tag{23a}$$

Equation (23a) suggests unitary and conservation of the model at COM (e.g., Figure 2e). The electron of a physical entity is non-abelian and its matrix of anticommutation is,

$$\left[ \psi_\alpha(\mathbf{x}, t), \psi_\beta^\dagger(\mathbf{y}, t) \right] = \delta_{\alpha\beta} \delta^3(\mathbf{x} - \mathbf{y}), \tag{23b}$$

where $\mathbf{x}$, $\mathbf{y}$ denotes the uncertainty principle into 3D space of linear time. Comparably this can be represented in the form,

$$\left\{ a_{\mathbf{p}}^r, a_{\mathbf{q}}^{s\dagger} \right\} = \left\{ b_{\mathbf{p}}^r, b_{\mathbf{q}}^{s\dagger} \right\} = (2\pi)^3 \delta^{rs} \delta^3(\mathbf{p} - \mathbf{q}). \tag{24}$$

where position, $\mathbf{p}$ and momentum, $\mathbf{q}$, are conjugate operators of virtual particles popping in and out of existence towards the emergence of real particle. In order not to violate unitary and constrain the dilemma of multiple entanglement, the existence of virtual particles is attributed to the devoid GS and the particle property to the occupied GS accommodating the shift in the electron's positions, $\psi_{0\rightarrow 3}$ in repetition. Into forward time towards the classical scale, only positive-frequency of Fourier transform is generated at COM (Figure 2d) such as [52],

$$\langle 0 | \psi(x) \bar{\psi}(y) | 0 \rangle = \langle 0 | \int \frac{d^3p}{(2\pi)^3} \frac{1}{\sqrt{2E_{\mathrm{p}}}} \sum_r a_{\mathrm{p}}^r u^r(p) e^{-ipx}$$

 doi:10.20944/preprints202210.0172.v18



$$\times \int \frac{d^3q}{(2\pi)^3} \frac{1}{\sqrt{2E_{\mathrm{q}}}} \sum_s a_{\mathrm{q}}^{s\dagger} \bar{u}^s(q) e^{iqy} \; |0\rangle. \qquad (25)$$

Equation (25) implies to the dominance of matter over antimatter for the spinor. The existence of antimatter is assumed by DBT within the space-time in situ of the atomic MP model.

## IV. Ontology of MP Model to Quantum Field Theory

This section explores the ontology of the MP model to QFT with respect to Dirac spinor and how this becomes relevant to both string theory of multidimensional space-time structure and loop quantum gravity of non-commutative spin tetrahedra. Some explanations on the Standard Model theory and Lorentz transformation are provided respectively in sequential order thereafter. All of them are briefly plotted in order to pave the path for further examinations the conventional way.

### *A. Dirac Spinors, String Theory and Loop Quantum Gravity*

The elliptical MP field is a closed form of a string. Its excitation is related to the electron of a point-particle. At the vertex of position 0, the electron assumes ZPE and mimics a monopole with polarization of the MP field of a dipole moment by DBT. Only at a spherical vertex point-boundary of COM, the electron-positron transition is attained for the emergence of real particle. The other accompanied vertices of the MP field mimic COM resemble virtual particles in a vacuum. The same is applicable to ionized MP model for the particle-hole resonance. Twisting and unfolding process by DBT instigates open ended strings and helical spin property (Figures 6a and 6b). The branes evolve from the electron's path at positions, $0 \rightarrow 3$ or $4 \rightarrow 8$ and this constitutes BOs of multidimensional space-time structure (see also Figure 1d). The vortex electron forms a solenoid of GS pair at different vibrational modes away from COM and these are quantized into $n$-dimensions (e.g., Figure 2c). When the electron's orbit is against clockwise precession, negative helicity or left-handedness is conceived (Figure 6c) and vice versa for positive helicity or right-handedness (Figure 6d). In the process, non-commutative spin network of dynamical triangulations for quantum space-time tetrahedral is generated and this relates to a fundamental aspect of loop quantum gravity. The electron-positron transition satisfies the relations [5], $\sum_j \hat{e}_j \hat{e}_j^T = [e_i e_j] = c_{ij}^k e_k$ in flat Euclidean space. The coupling of angular momenta at positions 1, 3 is transposed on positions 5, 7 and the resultant tensor component as expansion

Preprints.org (www.preprints.org) | NOT PEER-REVIEWED | Posted: 20 August 2025 doi:10.20944/preprints202210.0172.v18



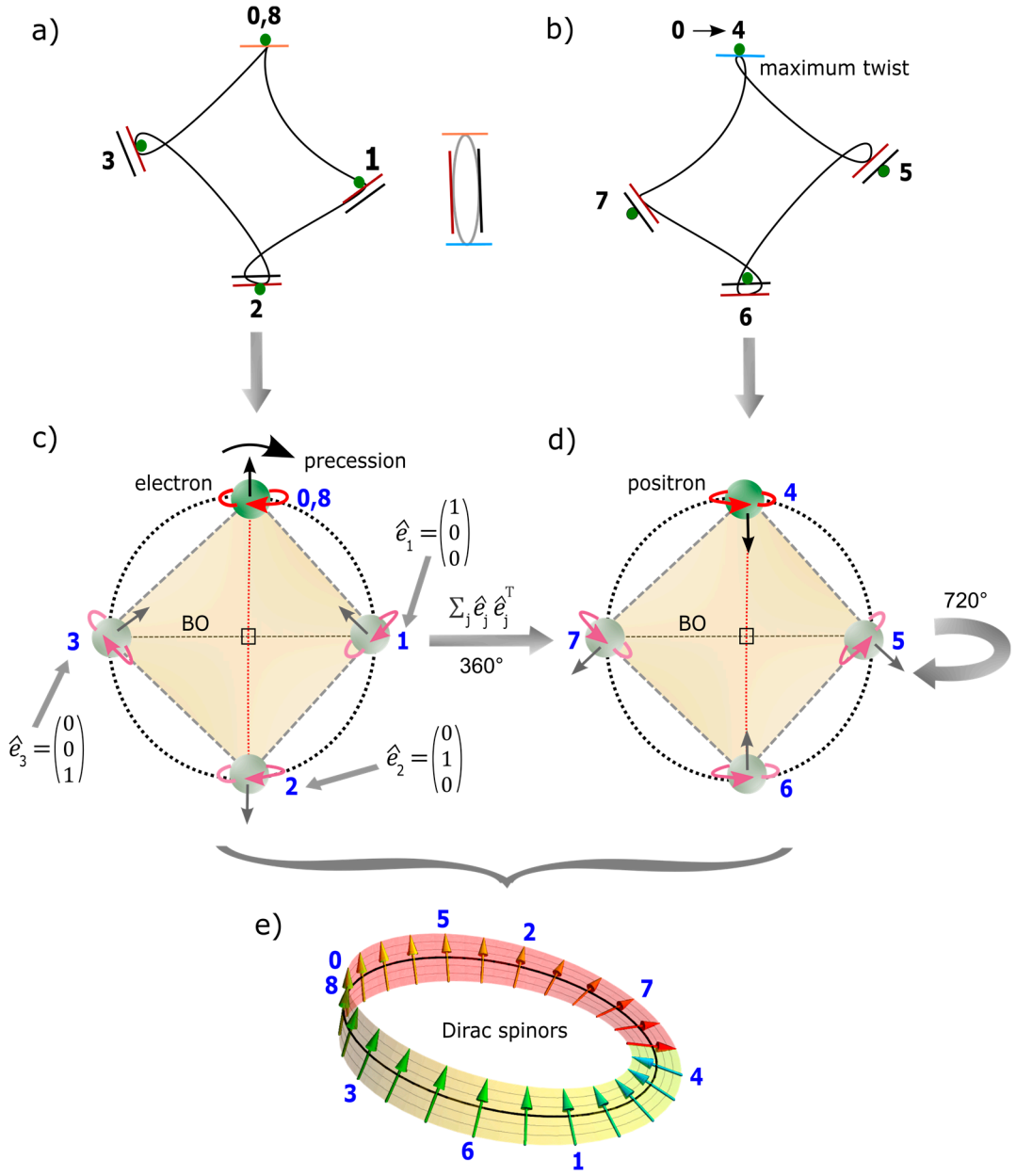


**Figure 6.** Relevance of the MP model to Dirac spinors, string theory and loop quantum gravity. (a) Away from COM of ZPE, the electron (green dot) or its particle-hole resonance assumes different vibrational modes. Light coupling to the electron's path appears tangential (colored lines) to the boundary of the MP field of Dirac's string (centered image). (b) Maximum twist and unfolding at COM allow for the emergence of antimatter in a superposition state. (c) Clockwise precession normalizes the electron's orbit to generate an electron of negative helicity or left-handedness and (d) positron of positive helicity or right-handedness. Both forms a network of non-commutative spin vectors of dynamical triangulations mimicking quantum space-time tetrahedra. The duplications of COM at the vertices from precession equates to multidimensional space-time structure. Transposition by DBT on the electron's path is converted to angular frequency of unit matrices, $\hat{e}_k$. (e) Cancelation of charges at conjugate positions, 1, 3 and 5, 7 from on-shell momentum offers close loops of BOs into 3D space for combined GS pair of irreducible spinors (see also Figure 3a). The electron of either spin up or spin down states is respectively assumed at positions 0 and 4. The slight tilt at position 4 is attained at COM, where energy loss from the electron-positron transition is of frictional force, $E = h\nu = g\beta B$. Image (e) is adapted from ref. [53].

coefficients, $c_{ij}^k$ are multiplied to the basis vector, $e_k$ of topological torus (see also Figure 2d). Angular frequency, $\omega^2 = k/m$ with the unit matrices, $\hat{e}_k$ into extra dimensions of COM at the vertex

 doi:10.20944/preprints202210.0172.v18



is assumed by clockwise precession of the MP field's vertices to induce an irreducible spinor (Figure 6e). The nucleus is confined to the center and its replication by COM into Minkowski space-time allows for the emergence of Higgs boson type (Figure 2c), with no distinction between helicity and chirality. Discreet symmetry breaking of charge conjugation and parity inversion or their combination is assumed by separation of chirality and helicity with respect to the particle's position in orbit. Quantum time is invariant for the MP model undergoing DBT and this can be differentiated from classical time (e.g., Figure 2d). At 720° rotation, combined CPT symmetry is restored in the absence of proton decay. The translation of 2D Euclidean space to 4D Minkowski space-time by rotation with COM at the spherical point-boundary is relevant to both the gravitational horizon and holographic principle. It provides the boundary between the quantum state and classical level. Furthermore, it incorporates Euler's formula for both hyperbolic and parabolic complex numbers with Pauli matrices, $i, 0, -1, 1$ assumed by vertical to horizontal polarization (e.g., Figures 2a–e). The matrices are traceless, Hermitian and of unitary within the spherical point-boundary. Clockwise precession of the vertices mimicking COM at the vertex of the MP field provides Hamiltonian spaces as earlier mentioned. These explanations form the basis for DBT within the MP model in accordance with the generic Dirac equation in the extended form,

$$\left(i\gamma^0\frac{\partial}{\partial t}+cA\frac{\partial}{\partial x}+cB\frac{\partial}{\partial y}+cC\frac{\partial}{\partial z}-\frac{mc^2}{\hbar}\right)\psi(t,\vec{x}), \tag{26}$$

where $c$ acts on the coefficients A, B and C and transforms them to $\gamma^1$, $\gamma^2$ and $\gamma^3$ with respect to the electron's shift in position, $\psi_{0\to3}$ of continuity. The exponentials of $\gamma$ are denoted $i$ for off-diagonal Pauli matrix for the light-cone of irreducible spinor and $\gamma^0$ to 0, 1 polarization states. Determinant –1 at position 4 of COM from time reversal preserves the volume and orientation of BO into $n$-dimensional space. The unitary matrices, $\sigma^i$ relate to oscillations from on-shell momentum of BO with anticommutative relationship, $e^+(\psi) \neq e^-(\bar{\psi})$ from the electron-positron pair (e.g., Figure 2c). The associated vector gauge invariance exhibits the following relationships,

$$\psi_L \to e^{i\theta L}\psi_L \tag{27a}$$

and

$$\psi_R \to e^{i\theta L}\psi_R. \tag{27b}$$

The exponential factor, $i\theta$ is given by the shift in the electron's position at an angle referenced to $z$-axis (Figure 5a). Exchanges of left- and right-handed Weyl spinor for the GS pair is given by the process,

$$\begin{pmatrix}\psi_L'\\ \psi_R'\end{pmatrix}=\begin{pmatrix}\psi_R(x)\\ \psi_L(x)\end{pmatrix}\Rightarrow\begin{matrix}\psi'(x')=\gamma^0\psi(x)\\ \bar{\psi}'(x')=\bar{\psi}(x)\gamma^0.\end{matrix} \tag{28}$$

Equation (28) conserves both local symmetry and global symmetry at COM by clockwise precession to induce Minkowski space-time. The usual properties of projection operators like: $L + R = 1$; $RL = LR = 0$; $L^2 = L$ and $R^2 = R$ can identify with the GS pair accommodating the shift in the electron's position by DBT. The unitary rotations of right-handedness ($R$) or positive helicity and left-handedness ($L$) or negative helicity are restored by electron's shift in position within the interchangeable GS pair. The helical symmetry from projections operators acting on the spinors are of the form,

$$P_L=\frac{1}{2}(1-\gamma_5) \tag{29a}$$

and

$$P_R=\frac{1}{2}(1-\gamma_5), \tag{29b}$$

 doi:10.20944/preprints202210.0172.v18



where $\gamma_5$ relates to $I$ matrices (Equation (8)) and this is incorporated by the eigenstates, $i$ from the electron shift in positions $0 \rightarrow 3$ in repetition. Equations (29a and 29b) assumes local symmetry for the conservation of the atomic model of Dirac spinor.

*B. Standard Model Theory*

Dirac spinor forms the basis of the Standard Model (SM) theory of particle physics. Thus, how the SM can be viewed from the geometry perspective of the MP model is plotted first by considering renormalization with respect to both harmonic oscillation and self-geometric structures (Figure 3a). This is followed by gauge symmetry of a stable nucleus (Figure 2e).

(i) Renormalization as a natural phenomenon

The SM of quarks and leptons of ±1/2 spin are quantized states of forces and these are mediated by gauge bosons of mostly neutrally charged, spin 1 as force-carrying particles. The four main forces are gravity, electromagnetism, weak and strong nuclear forces. The bosons for the three forces have been positively identified in experiments except for graviton of spin 2 particle. It is still not clear yet at what high energy regime, Planck scale is expected to emerge, where gravity becomes a dominant force in order to be reconciled into the SM as quite successfully done for the other three forces and particles identified so far. The pinnacle of the SM culminated in the discovery of Higgs boson as a proof to the existence of a proposed mass-giving mechanism. However, up till now, questions are still being raised on the nature of Higgs on how it bestows mass to the particles that includes both fermions and bosons. Without any decay of Higgs boson of a massive particle to leptons being concretely established, its decay to $W^{\pm}$ and Z bosons of the weak nuclear force has been positively identified [54]. For these bosons, the link to the electron and its cousins requires renormalization and at the least, fine-tuning in order to comply with the spin-charge of the hadrons from ionized hydrogen molecules. The process is deemed unnatural, where anthropic interventions are required in a series of mechanisms to agree with observations. If, however, the Higgs is assigned to COM (see also Figure 2a), it naturally relegates both renormalization and fine-tuning to a natural phenomenon of DBT. The variations in observed values of $\alpha$ from 1 part in a billion to 1 part in a trillion can be attributed to the electron-positron transition, $\psi_0 \rightarrow \psi_3$ of superposition states (see also explanations offered for Figure 3a). Thus, irrespective of the energy regimes, decoherence from photon coupling to the electron or its particle-hole resonance couplings can induce emergence of transient massive particles like $W^{\pm}$ and Z bosons of weak nuclear force (Figure 7a) and gluons of the strong nuclear force (Figure 7b).

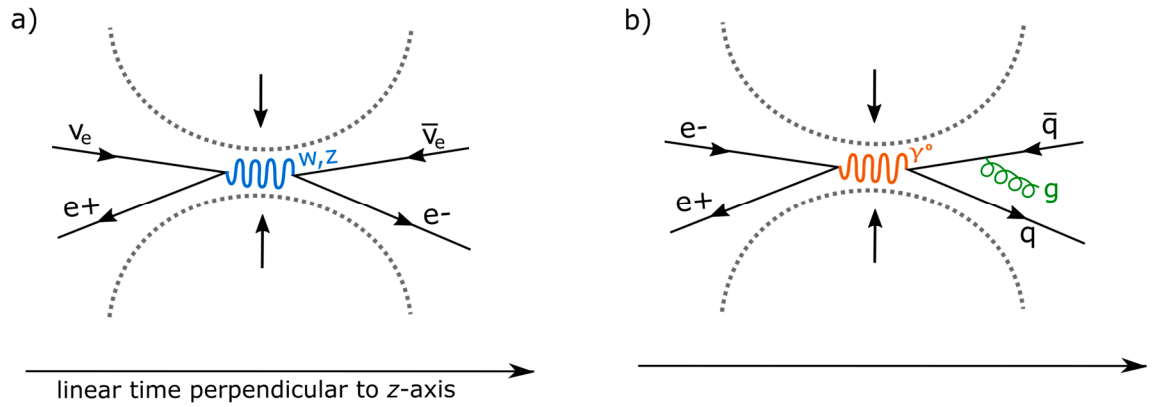


**Figure 7.** Coupling of ionized MP models at collisions are expected to mimic positively charged particle-hole resonance of the electron. These are compared to hadrons collisions of protonized hydrogen molecules in both (a) low energy and (b) high energy settings. At N = 4, the particle-hole resembles a four-component spinor of superposition states at N = 2. Renormalization at COM incorporates both harmonic oscillations (Figure 2c) and self-geometric structures (Figure 1a). Perturbation from on-shell momenta of Lamb shift is attained by

 doi:10.20944/preprints202210.0172.v18



magnetized light-MP model coupling (e.g., Figure 3a). Any outgoing Planck radiation is accentuated to reflect the energy regime of the experiments. Perpendicular translation to linear time from vertical to horizontal polarization or vice versa identifies with point-spread Green function (see also Figure 2d).

The polarization of photon coupling to matter as in the investigations of quantum information transfer like teleportation and cryptography [55] can relate to the four-component spinor at N = 4 and its superposition states at N = 2. Statistically, this can extend to both quarks under confinement and neutrinos and antineutrinos for energy conservation in the beta decay [56] of the electron for a range of energies observed in its continuous energy spectrum. Planck radiation from the electron-positron transition at COM of randomness can be accentuated to reflect three-jet events [57] of gluon color charge. Integer spins of 0 and 1 are assigned to COM at initial and completion of DBT with determinant −1 to positron emergence. The interchangeable GS pair of the irreducible spinor are shelf-geometric structures of harmonic oscillation mode (e.g., Figures 7a and 7b). Accentuation of perturbations from DBT is likely to hinder any observations of individual quarks in accordance with the property of asymptotic freedom (see also Figure 2c).

(ii) Gauge symmetry

The U(1) symmetry is global and is relegated to COM of perturbative state from the electron-positron transition by DBT. Its coupling tangential to light path is universal irrespective of where observations is made. This overrides the local SU(3) symmetry of the nucleus for quarks under confinement (Figure 2e). Under rotation or precession, the ladder operators for the local SU(2) symmetry are irreducible, $\binom{SU(2)}{n\times n} \neq \binom{SU(2)}{l\times l}\oplus\binom{SU(2)}{m\times m}$ and these relate to BOs of $n$-dimensions (e.g., Figure 1d). Translation by $\binom{SU(2)}{2\times 2}\oplus\binom{SU(2)}{2\times 2}$ to SO(4) is reflected by GS pair of 4D space-time. The particle's position of 2D, when $y = 0$, $z = x$ is a real number (Figure 2d) with the imaginary number at $x = 0$, $z = y$ (Figure 2e). Similarly, the SO(2) group is of the form [5],

$$\begin{pmatrix} cos\theta & sin\theta \\ -sin\theta & cos\theta \end{pmatrix} \cong \begin{pmatrix} 1 & \theta \\ -\theta & 1 \end{pmatrix} = I + \theta\begin{pmatrix} 0 & 1 \\ -1 & 0 \end{pmatrix}, \tag{30}$$

where, $\theta \in [0,2\pi]$ of complex phases confined to a hemisphere of 2D (e.g., Figure 1d). The orthogonal relationship by translation of quantum time to classical time suggests, $R \in SO(3)$ (see also Figure 2d). The SO(3) group rotation for integer spin 0 or 1 in 3D space is applicable to clockwise precession of the elliptical MP field and this can be expanded into a matrix series like,

$$\Pi_\mu(g_\phi) = \Pi_\mu\left[\begin{pmatrix} cos\phi & -sin\phi & 0 \\ sin\phi & cos\phi & 0 \\ 0 & 0 & 1 \end{pmatrix}\right] = \pm\begin{pmatrix} e^{i\frac{\phi}{2}} & 0 \\ 0 & e^{-i\frac{\phi}{2}} \end{pmatrix} = R_{xy}(\phi) \tag{31a}$$

and

$$\Pi_\mu(g_\theta) = \Pi_\mu\left[\begin{pmatrix} 1 & 0 & 0 \\ 0 & cos\theta & -sin\theta \\ 0 & sin\theta & cos\theta \end{pmatrix}\right] = \pm\begin{pmatrix} cos\frac{\theta}{2} & isin\frac{\theta}{2} \\ isin\frac{\theta}{2} & cos\frac{\theta}{2} \end{pmatrix} = R_{yz}(\theta), \tag{31b}$$

and

$$(g_\psi) = \Pi_\nu\begin{bmatrix} cos\psi & 0 & sin\psi \\ 0 & 1 & 0 \\ -sin\psi & 0 & cos\psi \end{bmatrix} = \pm\begin{pmatrix} 0 & e^{-i\frac{\phi}{2}} \\ e^{i\frac{\phi}{2}} & 0 \end{pmatrix} = R_{zx}(\psi). \tag{31c}$$

The electron (–) is out of phase against clockwise rotation and in phase for positron (+) in the generation of the helical property (e.g., Figures 6c and 6d). The exponential rise is by continuity of clockwise precession and its linear translation from linear light paths coupling tangential to the MP model at COM. The relationship of the irreducible spinor, $\Pi$ and its density is,

$$[\Pi(\hat{g})] = \rho(g). \tag{32}$$

 doi:10.20944/preprints202210.0172.v18



where $\rho$ is composed of algebraic structure ($pz$, $+p$ and $xp$) for vectorization, $V$ into $p$-dimensional space defined by $\alpha \wedge b$ within the model. Isomorphic rotation of 2 x 2 Pauli vector of SU(2) group is,

$$\pm\begin{pmatrix} cos\frac{\theta}{2} & isin\frac{\theta}{2} \\ isin\frac{\theta}{2} & cos\frac{\theta}{2} \end{pmatrix} = \begin{pmatrix} z & x-y_i \\ x+y_i & -z \end{pmatrix} = \begin{vmatrix} \xi_1 \\ \xi_2 \end{vmatrix} |-\xi_2 \quad \xi_1|, \qquad (33)$$

where $\xi_1$ and $\xi_2$ are Pauli spinors of rank 1 to rank 1/2 tensor relevant for Dirac matrices. The relationship, $R_{xy}(\phi) = e^{\theta}$ similar to Equation (31a) offers the matrix,

$$e^{\theta}\begin{bmatrix} 0 & -1 & 0 \\ 1 & 0 & 0 \\ 0 & 0 & 0 \end{bmatrix} = \begin{bmatrix} cos\theta & -sin\theta & 0 \\ sin\theta & cos\theta & 0 \\ 0 & 0 & 1 \end{bmatrix}. \qquad (34)$$

These equations provide the integral kernels of point-spread Greens function at COM as earlier suggested (see subsection IIc). The measurement outcomes are expected to be of superposition states for the electron-positron pair at transition akin to Stern-Gerlach experiment.

*C. Lorentz Transformation*

The COM of ZPE is dynamic and polarized by axial current from DBT to induce quantum time along $z$-axis. Any disturbance by observation shifts polarization from vertical to horizontal axes or vice versa. Linear transformation of perpetual motion then becomes [58],

$$x' = \gamma(x - vt/c^2) \qquad (35).$$

The corresponding 1D time is, $t' = \gamma(t - vx/c^2)$ with Lorentz factor, $\gamma = 1/\left(\sqrt{1 - v^2/c^2}\right)$ at $y' = y$ and $z' = z$. The GS pair is of Lorentz invariance under rotation, inversion and translation into space-time for $x = \gamma(x' - vt'/c^2)$ and $t = \gamma(t' - vx'/c^2)$. The Hermitian pair, $\psi^{\dagger}\psi$ is applicable to the electron-positron in superposition and these undergo Lorentz boost of the form,

$$u^{\dagger}u = (\xi^{\dagger}\sqrt{p.\sigma},\ \xi\sqrt{p.\bar{\sigma}}\,.\begin{pmatrix} \sqrt{p.\sigma}\xi \\ \sqrt{p.\bar{\sigma}}\xi \end{pmatrix},$$

$$= 2E_P\xi^{\dagger}\xi\,. \qquad (36)$$

Equation (36) is applicable to the Weyl spinors of the light-cones at the conjugate positions of either 1, 3 or 5, 7. The conversion to two component Dirac bispinor, $\xi^1\ \xi^2 = 1$ is assumed at COM. On this note, it is difficult to distinguish Dirac spinors from either Weyl or Majorana types. The corresponding Lorentz scalar for scattering from on-shell momentum of BO (Figure 3a) is,

$$\bar{u}(p) = u^{\dagger}(p)\gamma^0. \qquad (37)$$

By identical calculation to Equation (36), the Weyl spinors of chirality from the electron's position becomes,

$$\bar{u}u = 2m\xi^{\dagger}\xi. \qquad (38)$$

The pair of light-cones is invariant under Lorentz transformation and this can cater for special relativity for a body-mass in motion. The geometrical hyperbola of the light-cones is [59],

$$z - z' \equiv ct - ct' = tan^{-1}v/c = \alpha. \qquad (39)$$

The light-cone is linked to intrinsic angular momenta of the electron's path at positions 1 and 3 (e.g., Figure 1b) of the GS pair subjected to DBT. The light of electromagnetic radiation permeates space and its coupling to matter at the atomic level is limited to the electron-positron transition. These explanations can become important in the investigations of quantum information transfer in both teleportation and cryptography in contrast to entanglement for violation of lightspeed.

 doi:10.20944/preprints202210.0172.v18



## V. Ontology of MP Model to Space-Time Geometry

In this section, space-time fabric at the classical level is considered with COM reference frame of ZPE and its dynamics relegated to the spherical point-boundary of the MP model as mentioned earlier in the preceding sections. First, general relativity is intuitively plotted ensued by metric tensor and Lie group in subsequent order. The final subsection consists of space-time curvature for a body-mass of a planet in orbit of the sun akin to Rutherford atomic model in a multiverse of the MP models at a hierarchy of scales.

### *A. Space-Time Fabric of an Elliptical Orbit*

The framework of space-time fabric in an elliptical orbit or MP field of the electron is warped and unwarped by DBT and this is subjected to overall clockwise precession to generate a spherical MP model. The Cartesian coordinates of space-time, $t$, $x$, $y$, $z$ are assumed by spherical polar coordinates is, $\delta(z-z')=ct,\ r,\theta,\ \phi$ with respect to the electron's position. The former is relevant to Euclidean space-time of a clockface background projected in flat space of $n$-dimensions $\geq 1$ akin to Bohr model with distance between any two points being positive (e.g., Figures 1a and 5b). The latter is applicable to Minkowski space-time (e.g., Figure 1b), where a body-mass at a distance, $r$ of $n$-dimension acquires angular momentum, $\theta$ with respect to $z$-axis as arrow of time in asymmetry towards COM. The $n$-dimension of BO in degeneracy, $\phi_i$ is projected for the light-cone infinitely towards the center and it is cojoined by its counterpart in the opposite direction. Thus, singularity at the center can never be reached and but it can be mimicked by COM (e.g., Figure 2c). The moduli of vertices of COM from the MP field undergoing clockwise precession instigates the vortex electron's path of helical solenoid in the form,

$$B=\mu(\gamma^u\partial_v)\varepsilon L, \tag{40}$$

where $\mu$ is permeability of space, $\gamma^u\partial_{v=\theta,\phi}$ depicts BO into $n$-dimensions, $\varepsilon$ is electric current and $L$ is length equal to $z$-axis. By DBT, the path somewhat curves the pair of light-cones to resemble Riemann surface (Figure 8). Its component of Ricci tensor is attributed to the

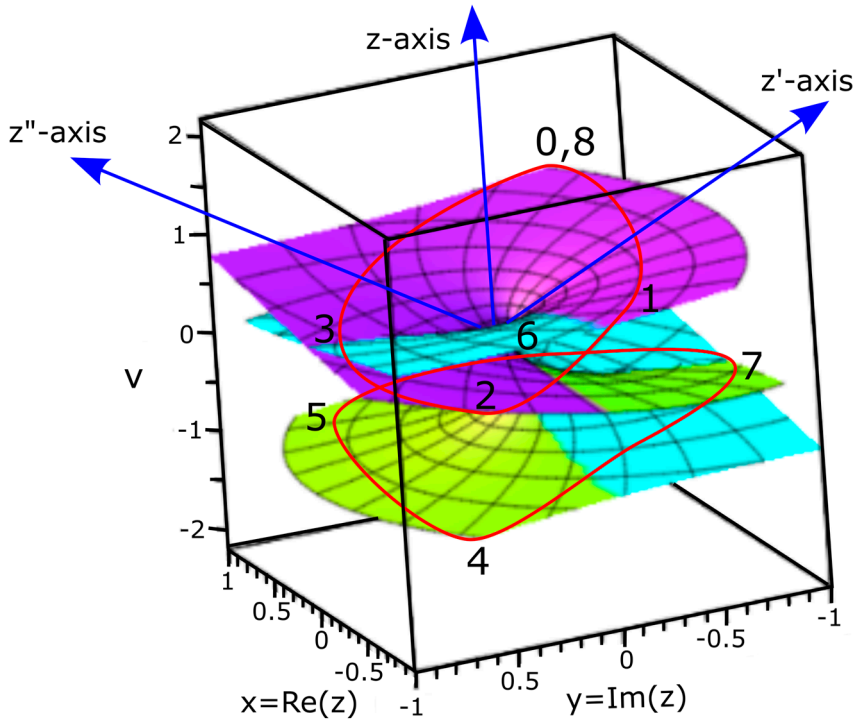

 doi:10.20944/preprints202210.0172.v18



**Figure 8.** A periodic Riemann surface for the cube-root function of 4D [60]. If interpreted within the MP model, the surface of 3D is warped and unwarped by DBT from the electron-positron transition (numbered positions, 0 to 8) within the levitated GS pair (red loops). The top GS combines with the hyperbolic surface of BO of a pair of light-cones (purple and turquoise colored) and the same applies to the bottom GS (greenish yellow and turquoise colored). Mixing and output under confinement is translated along *z*-axis of quantum time coinciding with classical time at COM (see also Figure 2e). The electron or its particle-hole of superposition states offer both real and imaginary potentials. The rotation of *z*-axis to *z′* and then *z′′* relates to clockwise precession of the MP field.

hypersurface of the manifolds of BO into *n*-dimensions resembling Riemannian manifolds (see also Figure 1d). The curvature of the manifolds from COM for combined GS pair is defined by Ricci tensor curvature, $R_{\alpha\beta} = 0$ (Figure 2c). The emergence of positive curvature, $R_{\alpha\beta} > 0$ and negative curvature, $R_{\alpha\beta} < 0$ for GS pair of oscillation mode is related to Minkowski space-time. The time-like region is referenced to the *z*-axis of a pair of light-cones and space-like region to BO of hyperbola geometry. The expansion of Ricci-type tensors along *z*- axis is of the form [61],

$$R_{\alpha\beta} \equiv R^{\gamma}{}_{\alpha\gamma\beta,} \qquad R_{\mu,\omega} \equiv R_{\alpha\beta}\mu^{\alpha}\omega^{\beta}. \tag{41}$$

In Equation (41), the Riemann tensor sign convention consists of four indices and these are very complicated and are not explored in this section. However, these could apply to the vortex electron's path for the Riemann surface comprised of manifolds of BO into *n*-dimensions (Figure 8). Contraction along *z*-axis towards the COM sustains the relationship,

$$R \equiv g^{\alpha\beta}R_{\alpha\beta}, \tag{42}$$

where $g$ is subset of space applicable to the metric tensor field and *R* is Ricci scalar. Examples of covariant and contravariant components of the inner products of $g$ are such as,

$$g_{ij} = \begin{pmatrix} 1 & 0 \\ 0 & sin^2\theta \end{pmatrix}, \qquad g^{ij} = \begin{pmatrix} 1 & 0 \\ 0 & \dfrac{1}{sin^2\theta} \end{pmatrix}. \tag{43a}$$

Its Levi-Civita connection has non-zero Christoffel symbols of the form,

$$\Gamma^{\phi}_{\phi\theta} = \frac{cos\theta}{sin\theta}, \qquad \Gamma^{\theta}_{\phi\phi} = -cos\theta sin\theta. \tag{43b}$$

Equations (43a and 43b) are applicable to the basis vector, $\vec{e}\theta$ and $\vec{e}r$ by continuity into space-time within a sphere (Figure 1c) and are reduced to plane wave solution, $e^{r\theta} = cos\theta + rsin\theta$ at the COM by coupling of linear light paths tangential to the model (e.g., Figure 2e). The combined metric for the two space-time spheres of Euclidean and Minkowski, $S^2$ at radius, *r* is given by,

$$ds^2 = r^2(d\theta^2 + sin^2\theta d\phi^2\,). \tag{44}$$

Equation (44) is applicable to the MP model of 4D quantum space-time.

*B. Space-Time Metric Tensor*

The body-mass such as an electron by homomorphism at COM is separated into two points of oscillation mode in a superposition state of entanglement (e.g., Figure 2c). This incorporates the relationship between the metric tensor and *I* given as [5],

$$g_{r\theta} = \begin{bmatrix} 1 & 0 \\ 0 & r^2 \end{bmatrix} \equiv I = \begin{bmatrix} 1 & 0 \\ 0 & 1 \end{bmatrix}, \tag{45}$$

where $g_{r\theta} = g_{\vec{v}.\vec{\omega}}$ is for speed with *v* by rotation and $\omega = 2\pi/\tau$ for angular frequency. The discrete Christoffel symbols, $\Gamma^{r}_{r\theta}$ or $\Gamma^{\theta}_{\theta r}$ and their variations by, $g_{r\theta}$ from clockwise precession transforms a body-mass in an elliptical orbit of 2D to 3D. Both the metric and stress-energy tensors appear symmetric so that $g_{\mu\nu} = g_{\nu\mu}$ and $T_{\mu\nu} = T_{\nu\mu}$. Each one of them requires 10 independent components

 doi:10.20944/preprints202210.0172.v18



from 4 x 4 matrices and these can be applied to MP model of 4D with quantum time aligned to z-axis. The relationship between the tensors in a rest frame is [62],

$$g_{\nu\mu} = kT_{\nu\mu} = \eta_{\alpha\beta} \tag{46}$$

where $k = 8\pi G/C^4$ is Einstein constant and $\eta_{\alpha\beta}$ is Minkowski space-time (Figure 1b). The space-time metric, $g_{\nu\mu}$ within two space-time spheres is comparable to Equation (44) in the form,

$$ds^2 = g_{\mu\nu}dx^\mu dx^\nu\,, \tag{47}$$

where $\mu\nu = 0,1,2,3$. The relevance of the indices for the electron's path suggests that $T_{\nu\mu}$ is the result of the presence of a body-mass in an elliptical orbit. The matrices garnered along its path are of the generalized form,

$$T_{\mu\nu} = \begin{pmatrix} T_{tt} & T_{tx} & T_{ty} & T_{tz} \\ T_{xt} & T_{xx} & T_{xy} & T_{xz} \\ T_{yt} & T_{yx} & T_{yy} & T_{yz} \\ T_{zt} & T_{zx} & T_{zy} & T_{zz} \end{pmatrix}. \tag{48}$$

Equation (48) can be dissected as follows [63]. Energy density, $T_{tt}$ is attributed to twisting and unfolding process of solenoid path by the electron-positron transition undergoing DBT. The momentum density, $T_{xt}\,T_{yt}\,T_{zt}$ or $T_{tx}\,T_{ty}\,T_{tz}$ for the plane wave solutions is referenced to orthonormal combination of quantum time to classical time of quantized Hamiltonian (e.g., Figure 2d). Shear stress like the rate of change in $x$-momentum in the $y$-direction is given by $T_{xy}$ and for $y$-momentum in the $z$-direction by, $T_{yz}$ and so forth. These identify with diagonal invariant rotation of the $x$-$y$ plane (e.g., Figure 9). The plane is part of the four 3-fold rotational axes for a body-mass at a lattice point of a cube. There are additional three 4-fold rotational axes on the faces and six 2-fold rotational axes at the edges. The negative pressure force, $T_{xx}$ $T_{yy}$ $T_{zz}$ directions are balanced out between the GS pair. Similarly, the matrix for $\eta_{\alpha\beta}$ such as,

$$\eta_{\alpha\beta} = \begin{bmatrix} 1 & 0 & 0 & 0 \\ 0 & -1 & 0 & 0 \\ 0 & 0 & -1 & 0 \\ 0 & 0 & 0 & -1 \end{bmatrix}, \tag{49}$$

can be equated to Equation (48) to forged the relationship, $\eta^{\alpha\beta} = T^{\mu\nu}$. This is relevant towards the merging of both Euclidean and Minkowski space-times within the MP model.

*C. Internal Structures by Lie Group Representation*

The rotation matrices of the type, $Rr_{yz}(\theta)$ and $R_{zx}(\theta)$ are attributed to clockwise precession of the MP field. Precession stages are referenced to $z$-axis at position 0 such that, $\langle z|z'\rangle = \delta(z - z')$ and these are transformed into linear time as plane wave solutions. The rotation matrix, $R_{xy}(\theta)$ intersects the BO of $n$-dimension defined by $\phi$. Such matrix is relevant to describe both integer and half-integer spins like, 0, 1/2 and 1 for complete rotation towards COM. How all these and others of the Lie group relate to the model are explored based on refs. [61,64]. The intuitive guide for the gauge group is provided in Figure 2e. The basis for vectors, matrices, tensors and Fourier transform are given in Figure 9. The electron of chirality is non-abelian. Only when

 doi:10.20944/preprints202210.0172.v18



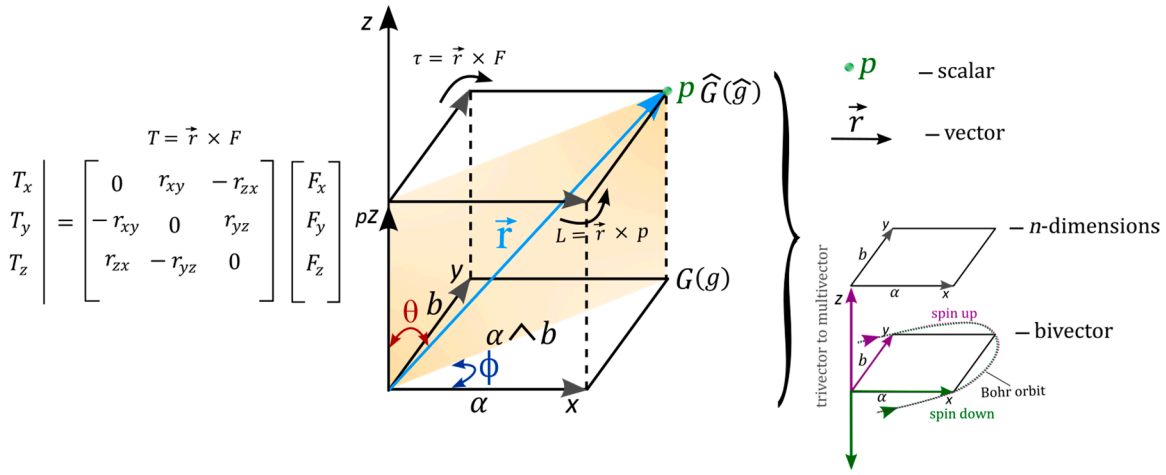


**Figure 9.** The basis of vectors to multivectors, matrices, tensors and Fourier transform for the electron's position (P) assigned to a cubic unit cell within the MP model akin to Figure 8 (see also Figure 1c). Fourier transform of tensor matrices is by commutation, $pZ$ to $Z$ and its reduction to COM allows for the interception of $z$-axis as quantum time into classical time (e.g., Figure 2d). The electron of a resultant vector, $\vec{r}$ for four 3-fold rotational axes (shaded orange plane) in 3D can relate to the vector space, $\vec{J} = \vec{L} + \vec{S}$ (see also Figures 4a and 4b). These are ascribed to 4-gradient Dirac operator, $\nabla$ for vectors to multivector of $n$-dimensions by the cube rotation about the $z$-axis. Stress-energy tensor of BO mimicking rotation into forward time, $\tau = \vec{r} \times F$ is balanced out by spin down of time reversal, $L = \vec{r} \times p$ attributed to the electron's orbit. The spin rotation matrices relevant to Clifford algebra are shown to the left. The half-integer spins of SU(2) group provide double cover (bivector) with shift in both $\theta$ and $\phi$ for BOs of topological torus (see also Figure 1d). These are relevant to the Lie group ladder operators, $G(g)$ and $\hat{G}(\hat{g})$. Some key features of the dimensional cube are exemplified to the right.

positioned at COM, it becomes abelian and sustains the global symmetry U(1). Away from the vertices, the particle's position is described by,

$$g \in G, \tag{50}$$

where $g$ is subset of space tangential to the manifolds of BOs and $G$ represents Lie group. For the emergence of BO, the charges are balanced out at the conjugate positions of, 1, 3 or 5, 7 (e.g., Figure 1d). Contravariant of space expansion by rotation, $\gamma^{\mu}$ at spherical lightspeed is balanced out by covariant measure, $\partial_{v}$ of the coordinates $\{\theta, \phi\}$ to induce a hyperbolic geometry. In this case, Equation (50) validates the operations,

$$g_{1,5} + g_{3,7} \in G \tag{51a}$$

and

$$g + (-g) = i, \tag{51b}$$

where $i$ is spin matrix for spin ±1/2 mimicking the electron's solenoid path within the GS pair (see also Figure 8). Anticommutation, $g_1 + g_3 \neq g_5 + g_7$ from electron-positron transition ($\pm\, g$) is transient for positions 0, 4 and is overridden by the commutation of electron-electron, $g_1 + g_3 = g_3 + g_1$ upon completion of DBT at positions, 0, 8. The hyperbolic surfaces of the light-cones are compacted orthonormal to isomorphic BOs (Figure 2e). Non-linear to linear sum of expansion coefficients to the particle position is, $|\psi\rangle = \sum_n C_n/a_n\rangle$. The inner product of $r$ is a scalar and at any two points by precession forms vectors such as,

$$\vec{r}_1 \,.\, \vec{r}_2 = |\vec{r}_1|\,|\vec{r}_2| cos\theta, \tag{52}$$

where the lengths and relative angles are preserved in a sphere (e.g., Figure 1c). By assigning rotation matrix, $R$ to Equation (52), the transposition is,

 doi:10.20944/preprints202210.0172.v18



$$(Rr_1)^T(Rr_2) = r_1^T r_2 I, \quad (53)$$

where the identity matrix, $I = R^T \times R$ by compaction of vector bundles is assumed in homogenous spaces of BO. The shift in both $\theta$ and $\Phi$ provides double cover of SU(2) for vector to multivectors (e.g., Figure 1d). Inhomogeneity is expected from the electron's position linked to the pair of light-cones. In a cube, $\vec{r}$ is diagonal of a four 3-fold axis in 3D and its matrices are defined by the Cartesian coordinates, $x$, $y$ and $z$ (Figure 9). Its bivector field resonates with $z/pz$ of integers modulo $p$ of prime along the $z$-axis. Translation of isomorphic cubes about $z$-axis are compacted linearly into classical time (e.g., Figure 2d). The process coincides with vertical to horizontal polarization or vice versa (Figure 2e). The Levi-Civita connection, $\hat{e}_\theta = \hat{e}_r$ offers the basis factors for any changes of square infinitesimals, $d\theta = dr$ for rotational matrix of the tensors. Its link to the vertex of a cube and light-cone is subjected to the four 3-fold axes of rotation by DBT. This generates a complex periodic Riemann surface for the GS pair (e.g., Figure 8) and provides an ideal scenario to explore space-time curvature initiated at COM.

*D. Space-Time Curvature*

Based on the descriptions of geometry offered for the MP model of 4D quantum space-time, how this could apply to a planet in orbit of the sun in a multiverse of the models at a hierarchy of scales is considered in this section. In Figure 10, an alternative interpretation of Einstein field equation presented with gravitation horizon assigned to COM at the spherical point-boundary.

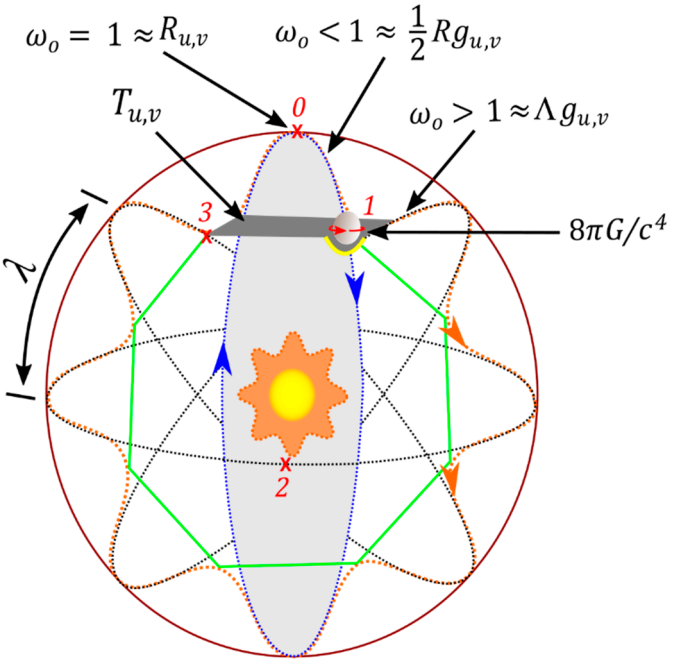


**Figure 10.** The components of Einstein field equation are applied to the geometry of the MP model of 4D space-time to incorporate a planet in orbit of the solar system in a multiverse at a higher hierarchy of scales. Space-time is warped and unwarped by shift in the body-mass, $\psi$ from positions $0 \rightarrow 3$ undergoing DBT. The emergence of angular momentum, $\vec{J}$ at position 1 and 3 mimics stress-energy tensor, $T_{\mu,\nu}$ with $\omega = 1$ by precession of the MP field. Space expansion by rotation, $\omega > 1 \cong \gamma^\mu$ is balanced out by contraction, $\omega < 1 \cong \partial_v$ from the electron's orbit. Hamiltonian of moduli space (green outline) of hypersurface generates Riemann curvature (yellow curve), $R_{\mu,\nu} = 1/2Rg_{\mu\nu}^{\lambda} - \Lambda g_{\mu\nu}^{\lambda}$ at the lattice points, 1 and 3 of a cubic unit cell (e.g., Figure 9). This can be woven into space network of fine fabric (Figure 8). The gravitational horizon (purple circle) is depended on the body-mass at the vertex of the MP field related to COM. Image adapted from ref. [34] and slightly modified.

 doi:10.20944/preprints202210.0172.v18



The model's relevance to perturbations from nonlinearity of differential gravitation acceleration, eccentricity of the reference orbit and its oblatenes in addition to the relative motion of the planet against the sun's gravity are complex phenomena [37]. These are attributed to both Newtonian gravity and general relativity. By assigning gravity to COM, some of these motions can relate to the process of DBT in a multiverse of the models at the classical scale. The gravitational horizon of other planets at the vertices of the MP field remains relative to the position of an observer stationed on Earth [65]. This considers multiple planets in orbit of the solar system to multielectron atom of multiple MP fields. The Earth's orbit at the vertex forms an aphelion with respect to the sun. At positions 2 and 6, the planet is perihelion to the sun. The COM integrates both Coulomb force and Newton's law of gravity, $F = G\frac{q_1 q_2}{r^2}$ , with $G = \frac{1}{4\pi\varepsilon_0}$ is offered by the dipole moment of DBT. Whether this could be linked to the vertical electric dipole from layered surface of Earth or sea [66] remains a possibility to interact with body-masses at a distance. For gravity alone cannot adequately account for the anomalous advances in Mercury's perihelion precession even with general relativity [67]. When interpreted within the MP model, first the process of DBT at COM will constantly variate the position of vertices of the MP field undergoing clockwise precession. Second, for a body-mass confined to an interchangeable hemisphere of GS type, there will be overlap to the cycles of elliptical loops in forming a sphere. Both of them are observed for Mercury's orbit, so the notion of matter curves space-time and space-time tells matter how to move is applicable to the model. Such suggestion mimics well studies [68] into the damping of the torque from electromagnetic coupling of core-mantle towards tidal dissipation to allow for free precession of Mercury's orbit. In a multiverse, the exertion of torque and damping is assumed at COM into Hilbert space and it is of the form [34],

$$8\pi G T_{\mu,\nu} \equiv i\hbar_{\mu,\nu}. \tag{54}$$

A major limitation in a multiverse is the scale of Dirac's string. If the body-mass from an electron is accentuated to correlate with a planet, then there is the possibility that Dirac's string should also become colossal. Whether this is beyond observations on instrumentations stationed on Earth presents an open ended question. One speculation is that the string is only an emergent property that comes into existence as the body-mass moves. If that is the case, then any infinitesimal spatial and temporal change becomes,

$$8\pi G \int_{-\infty}^{\infty} (dRdTdg)_{u,v} \equiv i \int_{-\infty}^{\infty} (d\Omega d\phi d\theta)_{u,v}. \tag{55}$$

Equation (55) offers an alternative version of Einstein's field equation with, $1/2\mathrm{R}g^{\lambda}_{\mu\nu} - \Lambda g^{\lambda}_{\mu\nu} = R_{\mu\nu}$ assumed at positions 1 and 3 at the vertices of the cube (Figure 9) and also at position 0 of COM. In this case, space-time singularities from dense matter with respect to quantum gravity at the center of mass is evaded. Instead, both negative and positive curvatures are generated about the COM such as the lattice points at positions 1 and 3 to induce diagonal rotations of helical solenoid mimicking Riemann surface (e.g., Figure 8). The same is applicable to body-masses in a multiverse of the models, where Coulomb attractive force is expected to stabilize it by polarization from DBT between two or many body-masses at a distance. Perhaps, the extent of the observable universe is limited to an elliptical cosmic microwave background resembling a MP field. How this can accommodate black hole, cosmic inflation, cosmological principle, dipole anisotropy, dark matter, dark energy and so forth has been previously inferred [34]. Similarly, a multiverse can also cater for the measurement problem, fine-tuning, gravity and enlarged vacuum fluctuations in an otherwise inflationary, homogeneous, isotropic and flat universe.

## VI. Conclusions

The ontology of the MP model for the hydrogen atom type is assumed on the basis that light-matter coupling is constrained to the electron's position in an orbit of an elliptical MP field undergoing clockwise precession to generate 4D quantum space-time. It offers an advanced version of Schrödinger's electron cloud model by incorporating the electron's spin-charge with its

 doi:10.20944/preprints202210.0172.v18



polarization assumed by DBT to generate a complex Dirac spinor. The COM relevant to Newtonian gravity is assigned to a specific spherical point-boundary and its dynamics appears compatible with many facets of physics from low to high energy regimes. The model is still largely speculative of a multiverse proposition at a hierarchy of scales by both perpetual motion and possible enlargement of a hidden colossal Dirac's string. The former offers Planck radiation of frictional force type from the electron-positron transition at COM by DBT at random. The latter is supposed to be an emergent property of a body-mass in motion. Perhaps, a miniature prototype can be constructed and its coupling to energized linear light path should be investigated at an energy more than Dirac's string (so it becomes undetectable) but less than the body-mass (to be detectable). This can be investigated for Lamb shift, hydrogen spectrum, spin-charge superposition states, wave-particle duality, entanglement, quantum gravity among others. Any successful outcomes could pave the path to explore the fundamentals of physics at the atomic level and this is worth further considerations.

**Data availability statement:** The modeling data attempted for the current study are available from the corresponding author upon reasonable request.

**Competing financial interests:** The author declares no competing financial interests.

## References


1. Lanciani, P. A model of the electron in a 6-dimensional spacetime. *Found. Phys.* 29(2), 251-265 (1999).
2. Nahin, P. *Dr. Euler's fabulous formula: cures many mathematical ills* (Vol. 52). Princeton University Press (2011).
3. Thaller, B. *The Dirac Equation*. Springer Science & Business Media (2013).
4. Sun, H. Solutions of nonrelativistic Schrödinger equation from relativistic Klein–Gordon equation. *Phys. Lett. A* 374(2), 116-122 (2009).
5. Nicol, M. Mathematics for physics: an illustrated handbook (2018).
6. Grandpeix, J. Y. and Lurçat, F. Particle Description of Zero-Energy Vacuum I: Virtual Particles. *Found. Phys.* 32(1), 109-131 (2002).
7. Blinder, S. M. Pauli Spin Matrices. Wolfram Demonstrations Project (2011).
8. Rovelli, C. Space is blue and birds fly through it. *Philos. Trans. Royal Soc. Proc. Math. Phys. Eng.* **376**(2123), 20170312 (2018).
9. Schrödinger, E. The general unitary theory of the physical fields. In *Proc. Roy. Irish Acad. Sect. A* **49**, 43-58 (1943).
10. Dürr, D. and Teufel, S. Bohmian mechanics. In *Bohmian Mechanics: The Physics and Mathematics of Quantum Theory* (pp. 145-171). Berlin, Heidelberg: Springer Berlin Heidelberg (2009).
11. Tittel, W. *et al*. Violation of Bell inequalities by photons more than 10 km apart. *Phys. Rev. Lett.* **81**(17), 3563 (1998).
12. Handsteiner, J. *et al*. Cosmic Bell test: measurement settings from milky way stars. *Phys. Rev. Lett.* **118**(6), 060401 (2017).
13. Krisnanda, T. *et al*. Observable quantum entanglement due to gravity. *Npj Quantum Infor.* 6(1), 12 (2020).
14. Rauch, D. *et al*. Cosmic Bell test using random measurement settings from high-redshift quasars. *Phys. Rev. Lett.* 121(8), 080403 (2018).
15. Weinberg, S. The trouble with quantum mechanics. *The New York Rev. Books*, January 19 (2017).
16. Chanyal, B. C. A relativistic quantum theory of dyons wave propagation. *Can. J. Phys.* 95(12), 1200-1207 (2017).
17. Trodden, M. Electroweak baryogenesis. *Rev. Mod. Phys.* 71(5), 1463 (1999).

 doi:10.20944/preprints202210.0172.v18




18. S. Santos, T. R. and Sobreiro, R. F. Remarks on the renormalization properties of Lorentz-and CPT-violating quantum electrodynamics. *Braz. J. Phys.* 46, 437-452 (2016).
19. Schiller, C. A conjecture on deducing general relativity and the standard model with its fundamental constants from rational tangles of strands. *Phys. Part. Nucl. Lett.* 50, 259-299 (2019).
20. Silagadze, Z. K. Mirror objects in the solar system?. *arXiv preprint astro-ph/0110161* (2001).
21. Rieflin, E. Some mechanisms related to Dirac's strings. *Am. J. Phys.* 47(4), 379-380 (1979).
22. Fox, T. Haunted by the spectre of virtual particles: a philosophical reconsideration. *J. Gen. Philos. Sci.* 39, 35-51 (2008).
23. Braccini, L. *et al*. Large spin Stern-Gerlach interferometry for gravitational entanglement. *arXiv preprint arXiv:2312.05170* (2023).
24. Atkinson, D. Does quantum electrodynamics have an arrow of time?. *Stud. Hist. Philos. Mod. Phys.* 37(3), 528-541 (2006).
25. Draper, P. and Rzehak, H. A review of Higgs mass calculations in supersymmetric models. *Phys. Rep*. 619, 1-24 (2016).
26. Khachatryan, V. *et al*. Search for microscopic black hole signatures at the Large Hadron Collider. *Phys. Lett. B* 697(5), 434-453 (2011).
27. Penrose, R. and MacCallum, M. A. Twistor theory: an approach to the quantisation of fields and space-time. *Phys. Rep.* 6(4), 241-315 (1973).
28. Smolin, L. How far are we from the quantum theory of gravity?. *arXiv preprint hep-th/0303185* (2003).
29. Li, K. *et al*. Quantum spacetime on a quantum simulator. *Commun. Phys.* 2(1), 122 (2019).
30. Cohen, L. *et al*. Efficient simulation of loop quantum gravity: A scalable linear-optical approach. *Phys. Rev. Lett.* 126(2), 020501 (2021).
31. van der Meer, R. *et al*. Experimental simulation of loop quantum gravity on a photonic chip. *Npj Quantum Inf.* 9(1), 32 (2023).
32. Machluf, S., Japha, Y. and Folman, R. Coherent Stern–Gerlach momentum splitting on an atom chip. *Nat. Comm.* 4(1), 2424 (2013).
33. Curiel, E. Singularities and black hole. *Stanford Encyclopedia of Philosophy* (2019).
34. Yuguru, S. P. Unconventional reconciliation path for quantum mechanics and general relativity. *IET Quant. Comm.* 3(2), 99–111 (2022).
35. Audoin, C. and Guinot, B. *The measurement of time: time, frequency and the atomic clock*. Cambridge University Press (2001).
36. Callender, C. and Huggett, N. (Eds.). *Physics meets philosophy at the Planck scale: Contemporary theories in quantum gravity*. Cambridge University Press (2001).
37. Jiang, F. *et al*. Study on relative orbit geometry of spacecraft formations in elliptical reference orbits. *J. Guid. Control Dyn.* 31(1), 123-134 (2008).
38. Bethke, S. Experimental tests of asymptotic freedom. *Prog. Part. Nucl. Phys.* 58(2), 351-386 (2007).
39. Sheppard, C. J., Kou, S. S. and Lin, J. The Green-function transform and wave propagation. *Front. Phys.* 2, 67 (2014).
40. Jaffe. R. L. Supplementary notes on Dirac notation, quantum states, etc. https://web.mit.edu/8.05/handouts/jaffe1.pdf (September, 2007).
41. Singh, R. B. *Introduction to modern physics*. New Age International (2008).
42. Bernauer, J. C. The proton radius puzzle–9 years later. In *EPJ Web of Conferences* (Vol. 234, p. 01001). EDP Sciences (2020).

 doi:10.20944/preprints202210.0172.v18




43. Samajdar, R. *et al*. Complex density wave orders and quantum phase transitions in a model of square-lattice Rydberg atom arrays. *Phys. Rev. Lett.* 124(10), 103601 (2020).
44. Machotka, R. Euclidean model of space and time. *J. Mod. Phys.* 9(06), 1215 (2018).
45. Durey, M. and Bush, J. W. Hydrodynamic quantum field theory: The onset of particle motion and the form of the pilot wave. *Front. Phys.* 8, 300 (2020).
46. Beenakker, C. W. J. Search for Majorana fermions in superconductors. *Annu. Rev. Condens. Matter Phys.* 4(1), 113-136 (2013).
47. Tumulka, R. Bohmian mechanics. In *The Routledge Companion to Philosophy of Physics* (pp. 257-271). Routledge (2021).
48. Bhaumik, M. L. The enigmas of fluctuations of the universal quantum fields. *arXiv preprint arXiv:2401.08638* (2023).
49. Burdman, G. Quantum field theory I_Lectures. http://fma.if.usp.br/~burdman (October, 2023).
50. Oshima, S., Kanemaki, S. and Fujita, T. Problems of Real Scalar Klein-Gordon Field. *arXiv preprint hep-th/0512156* (2005).
51. Peskin, M. E. and Schroeder, D. V. *An introduction to quantum field theory*. Addison-Wesley, Massachusetts, USA (1995).
52. Alvarez-Gaumé, L. and Vazquez-Mozo, M. A. Introductory lectures on quantum field theory. *arXiv preprint hep-th/0510040* (2005).
53. https://en.wikipedia.org/wiki/Spinor (updated February 2024).
54. Donoghue, J. F. The fine-tuning problems of particle physics and anthropic mechanisms, in *Universe or multiverse*, edited by B. Carr (Cambridge University Press, Cambridge, 2007) pp 231-246.
55. Lamas-Linares, A. Howell, J. C. and Bouwmeester, D. Stimulated emission of polarization-entangled photons. *Nature* 412(6850), 887-890 (2001).
56. Brown, L. M. The idea of the neutrino. *Phys. Today* 31(9), 23-28 (1978).
57. Berger, C. *et al*., and PLUTO Collaboration. Evidence for gluon bremsstrahlung in e+ e− annihilations at high energies. *Phys. Lett. B* 86(3-4), 418-425 (1979).
58. Naber, G. L. *The geometry of Minkowski spacetime*. Springer (2012).
59. Recami, E., Zamboni-Rached, M. and Licata, I. On a Time–Space Operator (and other Non-Self-Adjoint Operators) for Observables in QM and QFT. *In Beyond peaceful coexistence: The Emergence of Space, Time and Quantum* (pp. 371-417) (2016).
60. Jeffrey, D. J. Branch cuts and Riemann surfaces. *arXiv preprint arXiv:2302.13188* (2023).
61. Callahan, J. J. *The geometry of spacetime: an introduction to special and general relativity*. Springer Science and Business Media (2013).
62. Monteiro, R., Nicholson, I. and O'Connell, D. Spinor-helicity and the algebraic classification of higher-dimensional spacetimes. *Class. Quantum Gravity* 36(6), 065006 (2019).
63. Markley, L. C. and Lindner, J. F. Artificial gravity field. *Results Phys.* 3, 24-29 (2013).
64. Freed, D. S. *et al*. Topological quantum field theories from compact Lie groups. *arXiv preprint arXiv:0905.0731* (2009).
65. Melia, F. The apparent (gravitational) horizon in cosmology. *Am. J. Phys.* 86(8), 585-593 (2018).
66. King, R. W. and Sandler, S. S. The electromagnetic field of a vertical electric dipole over the earth or sea. *IEEE Trans. Antennas Propag.* 42(3), 382-389 (2002).

 doi:10.20944/preprints202210.0172.v18



67. Vankov, A. A. General Relativity Problem of Mercury's Perihelion Advance Revisited. *arXiv preprint arXiv:1008.1811* (2010).
68. Peale, S. J. The free precession and libration of Mercury. *Icarus*, 178(1), 4-18 (2005).